Journal of Materials Chemistry B

ROYAL SOCIETY OF CHEMISTRY

REVIEW

View Article Online
View Journal | View Issue

Cite this: J. Mater. Chem. B, 2024, 12, 3171

Electrospun organic/inorganic hybrid nanofibers for accelerating wound healing: a review

Sai Yan,[a] Yuqi Qian,[a] Marjan Haghayegh,[a] Yuhan Xia,[a] Shengyuan Yang,[a] Ran Cao *[ab] and Meifang Zhu[a]

Electrospun nanofiber membranes hold great promise as scaffolds for tissue reconstruction, mirroring the natural extracellular matrix (ECM) in their structure. However, their limited bioactive functions have hindered their effectiveness in fostering wound healing. Inorganic nanoparticles possess commendable biocompatibility, which can expedite wound healing; nevertheless, deploying them in the particle form presents challenges associated with removal or collection. To capitalize on the strengths of both components, electrospun organic/inorganic hybrid nanofibers (HNFs) have emerged as a groundbreaking solution for accelerating wound healing and maintaining stability throughout the healing process. In this review, we provide an overview of recent advancements in the utilization of HNFs for wound treatment. The review begins by elucidating various fabrication methods for hybrid nanofibers, encompassing direct electrospinning, coaxial electrospinning, and electrospinning with subsequent loading. These techniques facilitate the construction of micro–nano structures and the controlled release of inorganic ions. Subsequently, we delve into the manifold applications of HNFs in promoting the wound regeneration process. These applications encompass hemostasis, antibacterial properties, anti-inflammatory effects, stimulation of cell proliferation, and facilitation of angiogenesis. Finally, we offer insights into the prospective trends in the utilization of hybrid nanofiber-based wound dressings, charting the path forward in this dynamic field of research.

Received 22nd January 2024,
Accepted 4th March 2024

DOI: 10.1039/d4tb00149d

rsc.li/materials-b

1. Introduction

The skin, being the largest organ of the human body, serves as a crucial barrier protecting us from external threats. Beyond thwarting the invasion of bacteria, viruses, and other microorganisms, the skin plays a pivotal role in the regulation of the endocrine system.[1–3] Therefore, prompt treatment of skin damage is essential to prevent potential risks. Unfortunately, chronic wounds, such as diabetic foot ulcers and severe burns, often necessitate prolonged and advanced medical interventions, imposing substantial financial burdens on patients.[4,5] Conventional wound treatment strategies include autografts, allografts, and xenografts.[6] However, these methods suffer from limited availability, donor shortage, and the risk of immune rejections.[7–9] Consequently, advanced wound dressings that can replace partial functions of skin grafts and promote wound healing are highly desirable.

Wound dressings can be categorized into traditional options such as gauze, and newer alternatives including hydrogels, foams, and electrospun nanofibrous membranes.[10,11] Among them, electrospun nanofibrous membranes have gained considerable attention due to their high porosity, large specific surface area, and suitable mechanical strength.[12–14] Moreover, the nano-network structure of electrospun nanofibrous membranes closely resembles the natural extracellular matrix (ECM) of skin, making them promising candidates for wound treatment.[15–17] Additionally, electrospinning has evolved from single-fluid[18,19] to side-by-side[20,21] or coaxial,[22,23] triaxial[24,25] or even other multi-fluid derived structures including core–shell,[22] porous,[26] Janus[27,28] and even more complex and fine structures.[29,30] This offers a straightforward and practical method for utilizing a wide range of raw or modified materials, providing control over the nanofiber morphology and structure.[31–33] Furthermore, nanofiber membranes can function as carriers for the controlled delivery and release of biomolecules and drugs, expanding their application in the field of wound healing. In fact, some electrostatically spun wound dressings have already been commercially applied, such as FibriSEAL™ from St Teresa Medical, USA, PHOENIX™ from Nanofiber SOLUTIONS, USA, and Spincare® System from Nanomedic, Israel.

[a] State Key Laboratory for Modification of Chemical Fibers and Polymer Materials, College of Materials Science and Engineering, Donghua University, Shanghai 201620, P. R. China. E-mail: rancao@dhu.edu.cn, caoranaw@sina.com
[b] Shanghai Engineering Research Center of Nano-Biomaterials and Regenerative Medicine, Donghua University, Shanghai 201620, P. R. China

Skin primarily consists of water and an organic matrix, yet it also contains various inorganic elements, including calcium, iron, silicon, and zinc.[34,35] By incorporating these inorganic components with the organic matrix, the bioactivity of the hybrid nanofibrous membranes can be greatly enhanced.[36–39] As such, the use of electrospinning to create organic/inorganic hybrid nanofibers as novel wound dressings has seen rapid evolvement in recent years.

While many excellent review articles have explored the potential of hybrid materials for wound healing, they tend to focus on specific aspects, such as bioactive properties,[6] or the synthesis pathways of natural hybrids.[36] However, despite electrospinning being one of the most prevalent methods for preparing wound dressings, there is a notable absence of reviews summarizing recent progress in electrospun hybrid materials. Therefore, this review aims to bridge the gap by summarizing the fabrication and specific applications of hybrid nanofibers as wound dressings. We commence by discussing three typical preparation methods for electrospun organic/inorganic hybrid nanofibers, including direct electrospinning, coaxial electrospinning, and electrospinning with subsequent loading. The applications of electrospun organic/inorganic hybrid nanofibers are systematically summarized thereafter, including hemostasis, antibacteria, promoting cell proliferation and migration, accelerating angiogenesis and other direct (anti-inflammatory, antioxidant, and follicle regeneration) and indirect applications (drug loading) (Fig. 1). Moreover, potential mechanisms of the HNFs in promoting wound healing were discussed. Finally, we provide a comprehensive summary of the current state of research and offer insights into future development trends.

2. Preparation methods of HNFs

Electrospun organic/inorganic hybrid nanofibers (HNFs), combining the polymer matrixes with inorganic nanomaterials, possess a unique blend of superior properties from both components, rendering them attractive in various fields.[40] Furthermore, the electrospinning technique holds great promise for the cost-effective manufacture of continuous nanofibers. In essence, the HNFs can be categories into direct electrospinning, coaxial electrospinning, and electrospinning with subsequent loading (Fig. 2).

2.1. Direct electrospinning

Premixing organic matrixes and inorganic nanoparticles and then directly subjecting them to electrospinning (Fig. 2a) is the

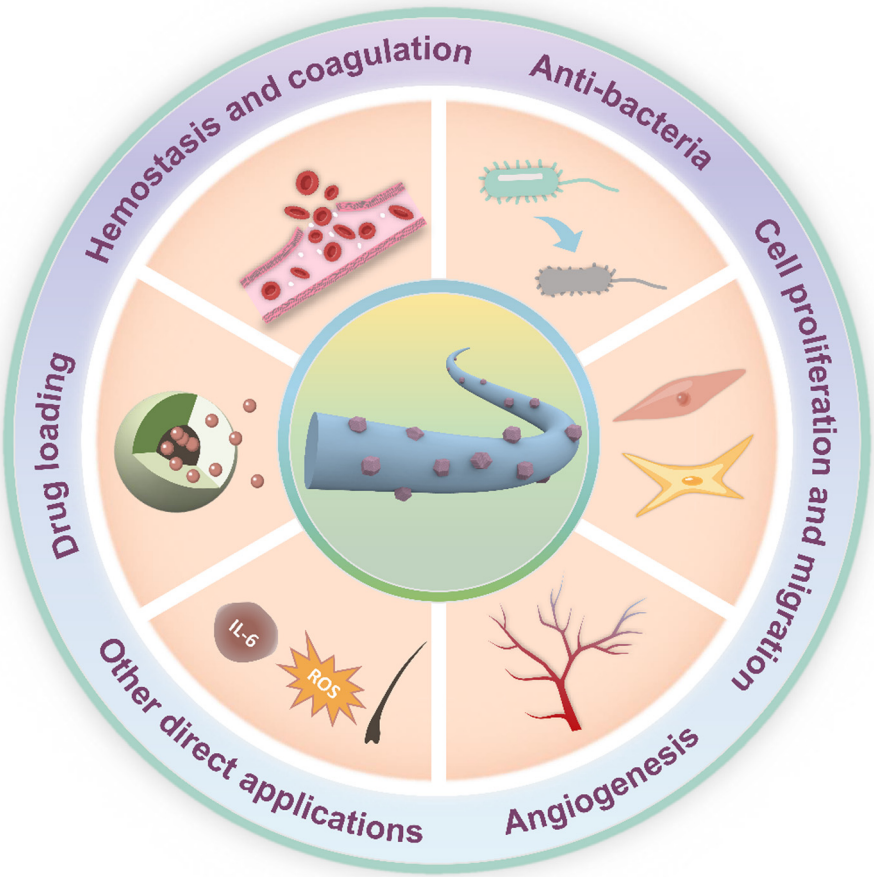

Fig. 1 Schematic diagram of electrospun organic/inorganic hybrid nanofibers (HNFs) for wound healing.

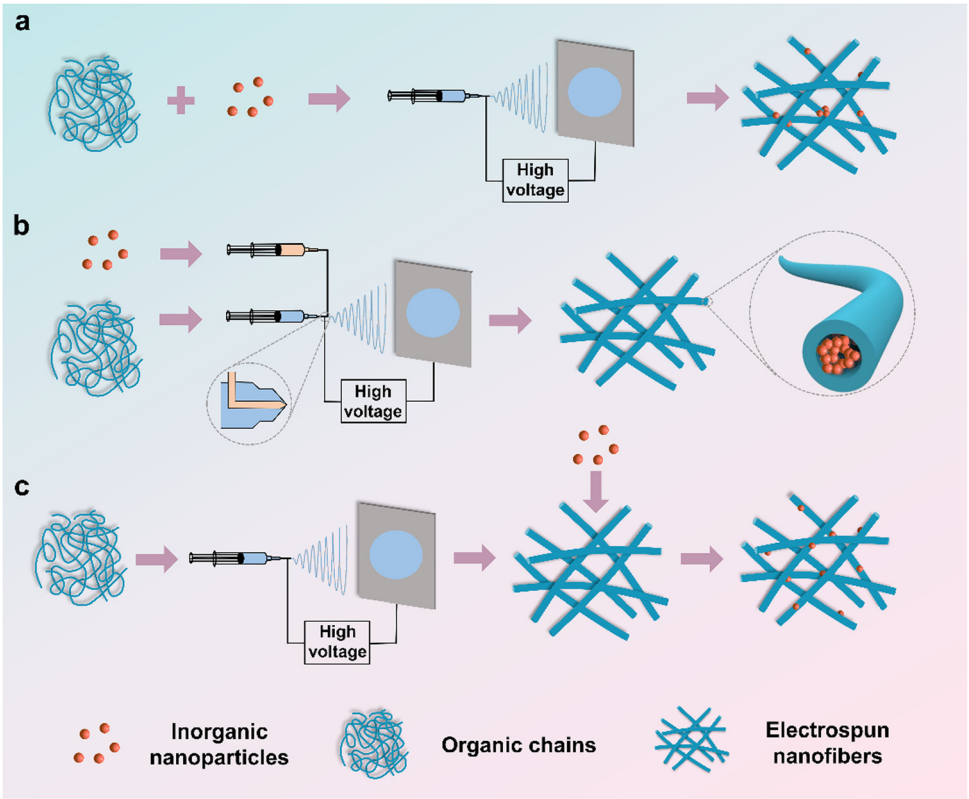

Fig. 2 Schematic illustration of the preparation methods of the electrospun organic/inorganic hybrid nanofibers (HNFs): (a) direct electrospinning, (b) coaxial electrospinning, and (c) electrospinning with subsequent loading.

simplest and most efficient method.[39,41] However, this method suffers from the inferior distribution of various components due to the fact that the high viscosity of polymer solutions retards the dispersion of inorganic nanoparticles. As a result, the inorganic nanomaterials are either dispersed on the nanofiber surface or encapsulated within the polymer nanofibers. For example, Chen *et al.*[42] physically mixed melatonin and Fe_3O_4 magnetic nanoparticles (Fe_3O_4-MNPs) with polycaprolactone (PCL) pellets in a solvent mixture of *N*,*N*-dimethylformamide (DMF) and dichloromethane (DCM). The obtained hybrid nanofibers acted as artificial nerve catheters for repairing nerve injuries.

2.2. Coaxial electrospinning

Coaxial electrospinning involves constructing core–shell nanofibers by using a multi-channel needle, where the core solution typically contains inorganic nanoparticles dissolved in a solvent or polymer solution, while the shell solution is another polymer solution (Fig. 2b).[32,43,44] This method allows the simultaneous electrospinning of core and shell solutions using a coaxial needle. Mahdieh *et al.*[45] fabricated antibacterial sheath–core fibers through coaxial electrospinning, using citrate-coated silver nanoparticles (AgNPs) dispersed in sodium citrate aqueous solution as the core solution and the shell solution comprising ZnO particles, polycaprolactone (PCL), and polyethylene glycol (PEG) in a chloroform/DMF mixture. The superiority of this method lies in the controllable release of the inorganic components or drugs in the core layer.[46] Nevertheless, the coaxial electrospinning process is complicated, and the compatibility of the core–shell solution limits the choice of materials.[46,47]

2.3. Electrospinning with subsequent loading

In this method, a pre-electrospun nanofibrous membrane is immersed in inorganic materials where the latter forms nanoparticles on the surface of the former (Fig. 2c). Rivero *et al.*[48] combined poly(acrylic acid) (PAA) with β-cyclodextrin (β-CD) to create nanofibrous membranes *via* electrospinning. The nanofibrous membranes were subsequently immersed in a silver nitrate solution, resulting in Ag^+ bonding to the carboxyl group of PAA. *Via* reducing Ag^+ with dimethylamine borane (DMAB) solution, Ag nanoparticles were successfully decorated on the nanofibrous membrane. The post-loading method ensures the even distribution of inorganic nanomaterials only on the surface of nanofibers.[49] However, this method requires suitable synthesis conditions for both organic and inorganic materials, and achieving precise control of the particle size and loading rate of inorganic materials is a challenge.

3. Mechanisms of the HNFs in accelerating wound healing

The efficacy of HNFs in expediting wound healing can be categorically delineated into two primary mechanisms. Firstly, the hierarchical nanostructures arising from the interplay of

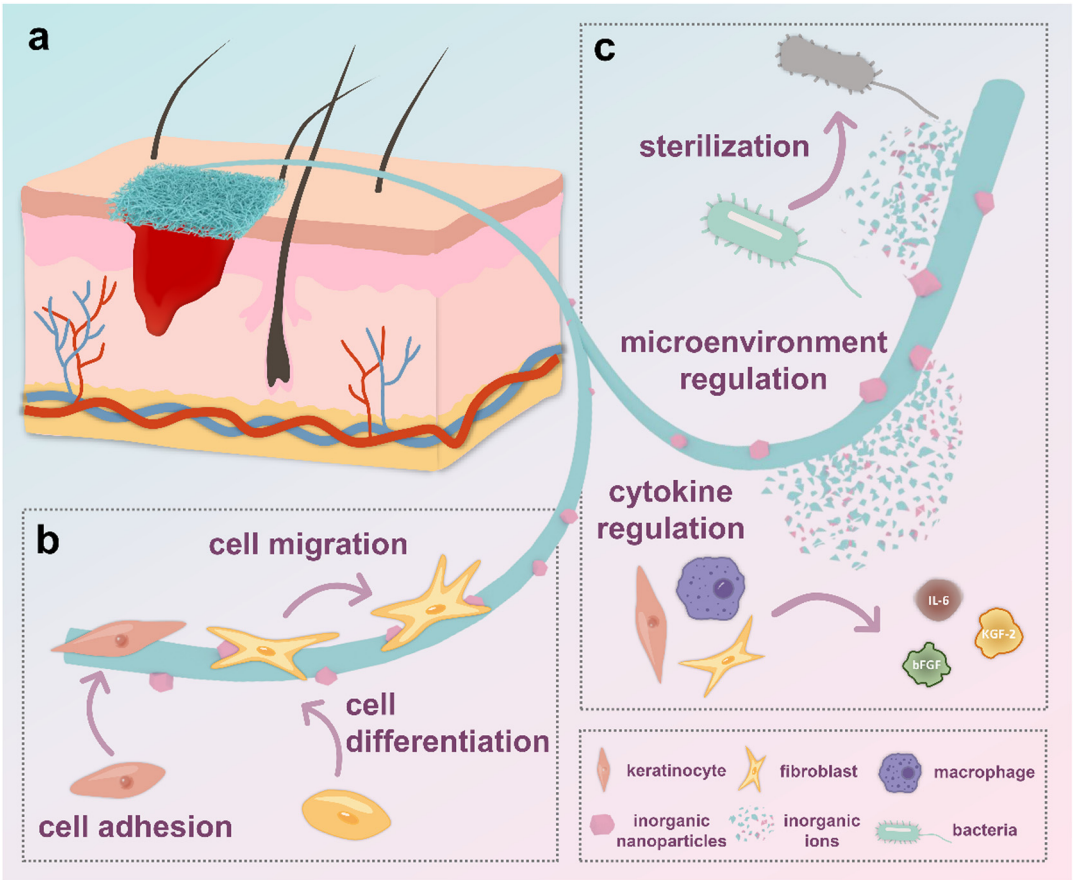

Fig. 3 Illustration of HNFs in promoting wound healing: (a) illustration of HNFs covered on the wound area; (b) illustrations of how hierarchical nanostructures play a pivotal role in directing cell behavior; and (c) illustrations of how the release of active substances regulates both the microenvironment and cell behavior around the wound.

organic fibers and inorganic nanoparticles serve to intricately guide cellular behavior. Secondly, the controlled release of bioactive substances such as ions from the HNFs actively modulates the microenvironment surrounding the wound site, thereby orchestrating a concerted influence on cellular behavior (Fig. 3).

3.1. Hierarchical nano-structures

It is a notion long acknowledged in scientific literature that the microstructure exerts a profound influence on cells and tissues.[50,51] The introduction of nanoparticles allows the electrospun nanofiber network to form a hierarchical nanostructure, which leads to increased surface roughness, and provision of better sites for cell adhesion.[52,53] Consequently, cell shapes and morphologies can be tuned according to the distribution of nanoparticles (Fig. 3b). Moreover, mechanical stimulation caused by the nanoparticles allows cells to enhance phagocytosis, accompanied by improved cellular viability. To some extent, this simulation provides an optimistic impact on the regulation of cell differentiation.[54,55] Besides, it is believed that the engineered uneven roughness surface can accelerate the spatial and temporal alternation between the extension of the pseudopods in the head of the cell, and the contraction of the tail of the cell body. As a result, cells tend to migrate faster, thus accelerating wound closure.[54,56] Wu and colleagues[57] prepared hierarchical nanofiber scaffolds with controllable micropattern substrates (squared-shaped, hole shaped, strip-shaped and hexagon shaped) and bioglass nanoparticles. Consequently, a 2-dimensional patterned structure with 300–400 μm variation, 1-dimensional fibers with the diameter in the range of 500–1000 nm, and the surface of individual nanofibers was composed of 0-dimensional bioglass nanoparticles (approximately 30 nm) were prepared. They observed that the layered micro-nanostructures and nano bioglass in the scaffold could work together to improve the efficiency of wound healing and re-epithelialization. Their research shows that electrospun nanofibers with square-shaped structures showed better healing efficiency due to its high porosity. In addition, bioglass nanoparticles smaller coated on the nanofibers are believed to promote the preferential adsorption molecules such as hyaline, which plays a crucial role in stimulating cell adhesion. Similarly, Lin *et al.*[54] prepared a hierarchical micro/nanofibrous scaffold incorporated with curcumin and zinc ion eutectic metal organic frameworks (ZIF-8) by using an electrospinning and crystal engineering method. Compared with the control group, these

microscopic/nanofibrous scaffolds increase the number of antennae and diffusion area of the cells, significantly affecting cell adhesion and migration. As can be seen from the above examples, hierarchical nano-structures constructed by nanofibers and nanoparticles have important implications for cell behavior and even wound healing.

3.2. Active substance release

In addition to their role in fostering hierarchical nanostructures, HNFs contribute to the promotion of wound healing through the release of active substances into the humoral environment (Fig. 3c). Those active substances such as ions exhibit versatility, with some inducing cells to generate cytokines, thereby expediting the wound healing process.[55,58,59] Besides, certain active substances contribute to the production of nutrients or modify the microenvironment through chemical reactions. For example, the generation of oxygen by nanoparticles can accelerate angiogenesis.[60,61] Furthermore, inorganic nanoparticles possessing charges or specific electron-pairing active sites on their surfaces can selectively bind to cells or other substances.[62,65,66] It should be noted that some inorganic nanoparticles also shows antimicrobial activity by releasing ions or having chemical reactions.[67,68] A number of specific experimental reports support these views. Augustine *et al.*[69] reported that the prolonged effect of endothelial cell proliferation and cell density increase is attributed to the slow and sustained release of europium hydroxide from the hybrid nanofiber scaffold. Ning and colleagues[70] demonstrated that their Ag-MOF hybrid electrospun scaffolds showed excellent antibacterial activity due to the slow release of Ag^{+} ions. The previously mentioned hierarchical micro/nanofibrous scaffold incorporated with ZIF-8 prepared by Lin *et al.* also showed a sustained release of curcumin and Zn^{2+}, contributing to the scaffold's increased cell proliferation, anti-inflammatory performance and antioxidant capacity.[54]

4. Applications of HNFs in wound healing

The wound healing process can be divided into four essential stages: hemostasis, inflammation, cell proliferation and migration, and maturation.[71–73] Different hybrid nanofibers have been developed to address specific requirements during each stage of wound healing. For example, the initial stage necessitates hybrid nanofibers with hemostatic and antibacterial properties.

4.1. Hemostasis and coagulation

Hemostasis is a prerequisite for the wound healing process. Inorganic materials such as montmorillonite, kaolinite, halloysite, and palygorskite have demonstrated the ability to accelerate hemostasis by actively stimulating the body's endogenous coagulation factors and facilitating the aggregation of blood cells.[74,75] However, a drawback of using the powdered form of the inorganic materials is their challenging aggregation and removal, which could potentially hinder the subsequent stages of wound healing.[75–78] Therefore, the combination of electrospun nanofibers and inorganic hemostatic powder is a promising method for improved hemostatic performance.[62] Moreover, nanofiber membranes, owing to their high flexibility, skin-friendly properties, and finely tuned pore size distribution, are proven to be effective in staunching blood exudation.[79–81]

4.1.1. Clay mineral nanoparticle based HNFs. Clay mineral materials such as montmorillonite are frequently employed in the preparation of organic/inorganic hybrid nanofibers for wound hemostasis.[62,65,82,83] Zhang and colleagues[62] prepared various nanoclay-based electrospun membranes (NEMs) (Fig. 4a) by incorporating sheet-like kaolinite (morphology is shown in Fig. 4b), tube-like halloysite, and rod-like palygorskite nanoparticles into polyvinylpyrrolidone (PVP) solution. Comparative analysis revealed that the hybrid electrospun membrane containing 60 wt% kaolinite (KEM1.5) exhibited the most efficient and rapid hemostatic performance, as demonstrated in both *in vitro* and *in vivo* studies. Delyanee *et al.*[65] enhanced the hemostatic performance by modifying halloysite nanotubes (HNT) using poly(amidoamine) (PAMAM) dendrimers (HNT-PAMAM). These functionalized HNTs were combined with poly(lactic acid) (PLA) to produce hybrid nanofibers *via* electrospinning. The results indicated that the hybrid nanofibers significantly accelerated blood clotting, attributed to the clay mineral materials' negative surface charge, which promotes coagulation by activating the endogenous coagulation pathway involving factor XII and platelets. Moreover, the synergistic effect of these nanofiber membranes physically blocked the bleeding point, further improving the hemostatic performance.

4.1.2. Metal-derived nanoparticle based HNFs. In addition to clay mineral hemostatic materials, a variety of metals or metal compounds have demonstrated hemostatic and coagulation effects. For instance, aluminum chloride ($AlCl_3$), a common chemical hemostatic agent, effectively stops bleeding by precipitating proteins, blocking tiny blood vessels, and constricting blood vessels.[84] Nasser *et al.*[63] fabricated a series of electrospun poly(L-lactic acid) (PLLA)/$AlCl_3$ nanofibrous membranes (Fig. 4d), with 30% w/w AlCl3 (MAC30) exhibiting the most effective hemostatic performance (morphology is shown in Fig. 4e). Notably, the PLLA nanofibrous membrane loaded with 30% w/w $AlCl_3$ (MAC30) demonstrated a substantial reduction in blood coagulation time (279 seconds), achieving a remarkable 80% reduction compared to conventional gauze bandages (Fig. 4f). This outcome underscores the superior hemostatic performance of the MAC30 membrane. In addition, the blood absorption capacity (the ratio of the weight of blood absorbed by the sample within 2 min to the original weight of the sample) of MAC30 was 178% higher compared to conventional gauze bandages and was even higher than that of polylactic acid nanofibers loaded with gentamicin sulfate and lidocaine hydrochloride (MAC10GS10LHc10).

Additionally, calcium, an essential element in hemostasis, functions as coagulation factor IV, accelerating thrombosis formation by increasing the polymerization rate of the fibrin monomer, and vascular contraction.[64] Moreover, calcium accumulating in the vascular smooth muscle cells can trigger vascular contraction, facilitating fast hemostasis. Yu *et al.*[64]

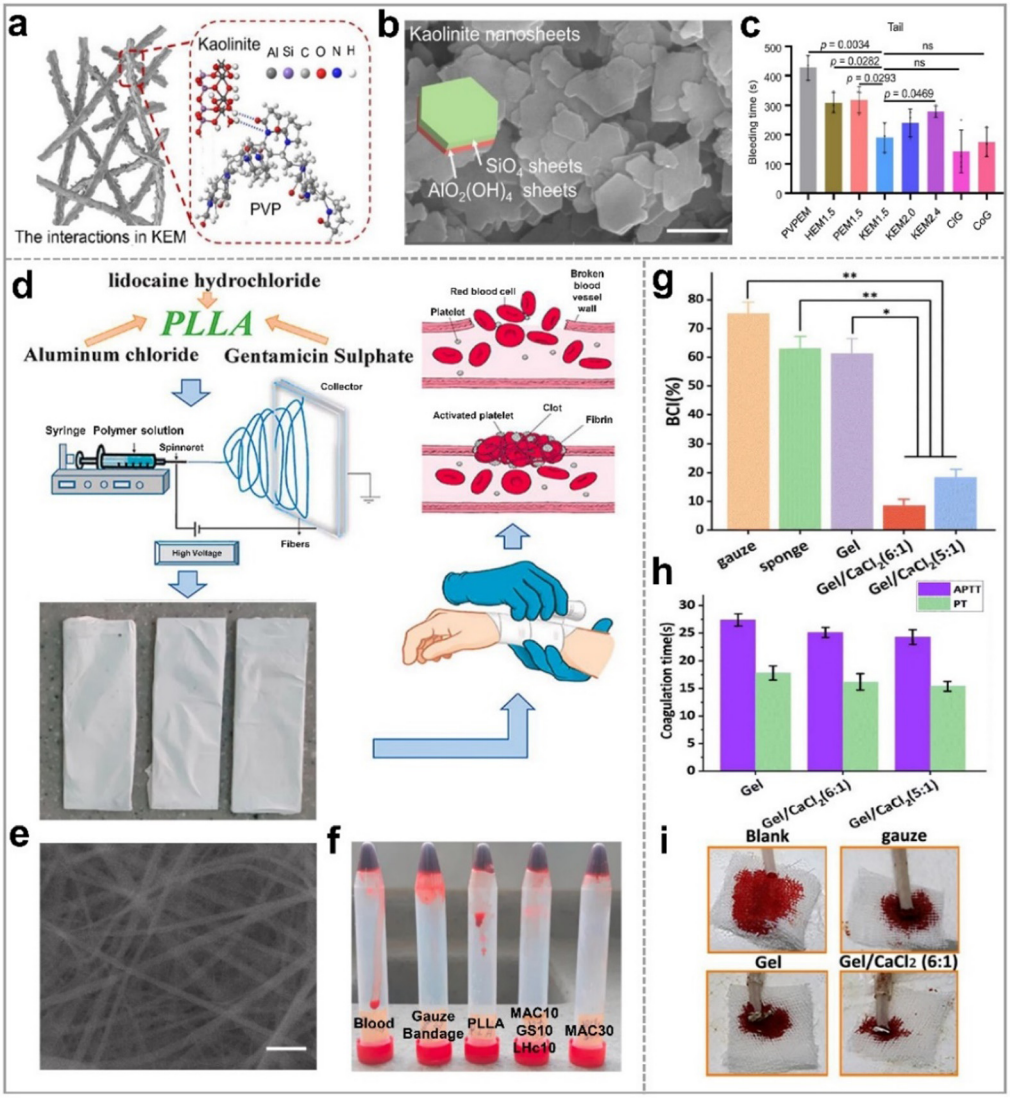

Fig. 4 Nanoclay-based electrospun membranes for hemostasis of wounds; (a) illustration of kaolinite/PVP nanofibers. (b) Scanning electron microscope (SEM) image of kaolinite (scale bar, 500 nm); (c) the bleeding time of the wounds treated with NEMs in rat-tail amputation hemostasis model; reproduced with permission,[62] CC BY 4.0. (d) Schematic illustration of the electrospun PLLA/$AlCl_3$ for hemostatic application; (e) SEM image of PLLA nanofibrous membrane loaded with 30% w/w $AlCl_3$ (scale bar, 2 μm); (f) optical photo of the blood clotting effect of five samples; reproduced with permission.[63] Copyright 2021, Elsevier. (g) BCI of gauze, gelation sponge, gelatin (Gel), and gelatin/calcium chloride electrospun nanofibers; (h) APTT and PT of Gel, Gel/$CaCl_2$ (6 : 1), and Gel/$CaCl_2$ (5 : 1) nanofibrous membranes; (i) tail vein hemostasis of mice treated with different samples; reproduced with permission.[64] Copyright 2023, Royal Society of Chemistry.

employed gelatin and calcium chloride as raw materials to prepare a hemostatic wound dressing (Gel/$CaCl_2$) through electrospinning. Hemostatic properties of calcium-doped nanofiber membranes are evident in the blood-clotting index (BCI) (Fig. 4g), activated partial thromboplastin time (APTT) and prothrombin time (PT) values of Gel/$CaCl_2$ and other samples (Fig. 4h). Furthermore, images of tail vein hemostasis in mice (Fig. 4i) underscore the effectiveness of these membranes. Notably, the Gel/$CaCl_2$ membranes with varying contents of gelatin and calcium chloride displayed BCI values of 8.57% and 18.4%, respectively, significantly lower than those of the gelatin nanofiber (Gel) membranes. Besides, the APTT value of Gel/$CaCl_2$ decreased by about 28 s compared with that of Gel, indicating that the addition of calcium ions improved the hemostatic ability of nanofiber membranes in an exogenous pathway. With a mean hemostatic time of 289 seconds and minimal blood loss (0.06 g), the Gel/$CaCl_2$ (6 : 1) membrane outperformed commercially available gauze (698 s, 0.31 g), blank control (846 s, 0.63 g), and Gel membranes (304s, 0.36g). In addition, silver,[85] zinc,[86] and other nanoparticle-based hybrid electrospun nanofibers have also exhibited exceptional hemostatic and coagulation properties.

4.2. Anti-bacterials

Wound healing is a protracted process during which bacteria can infiltrate the wound site, leading to infections – a

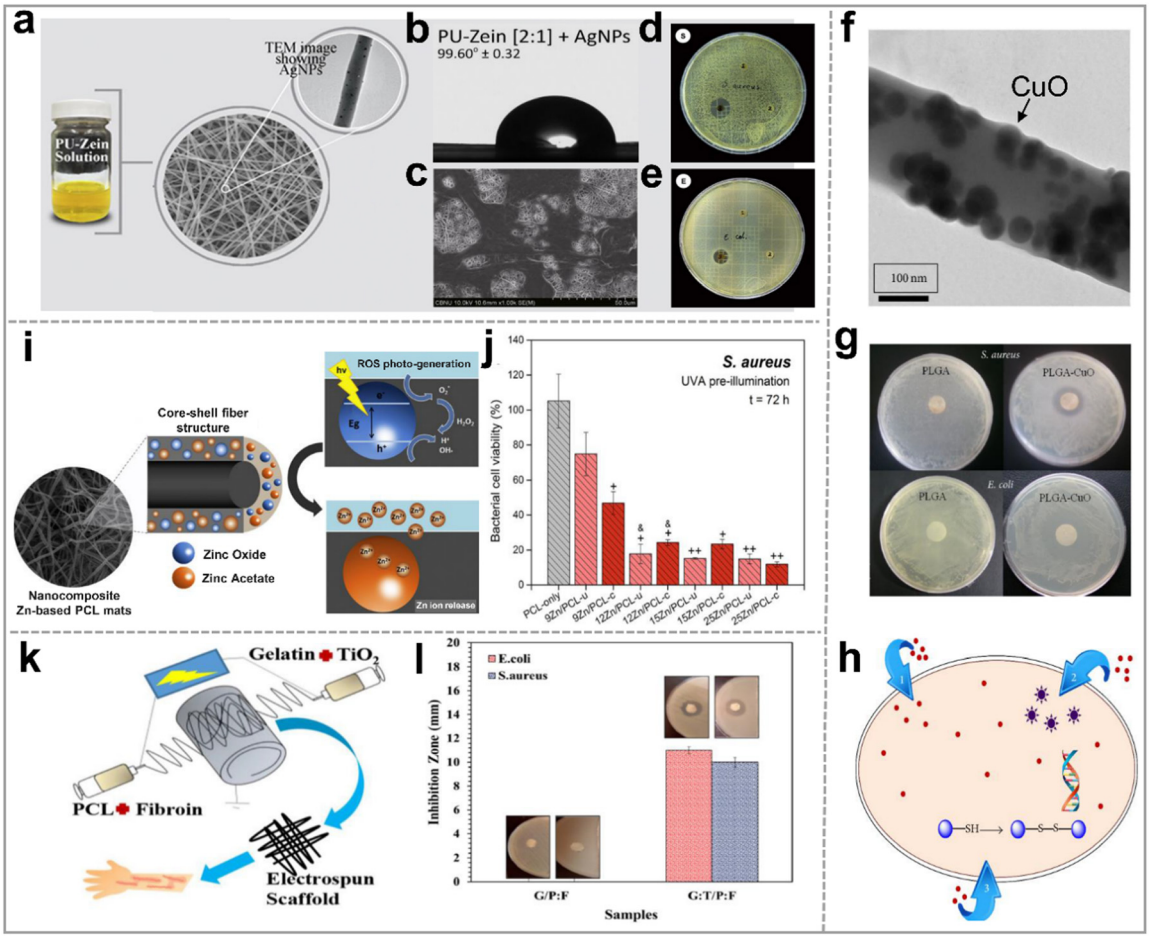

Fig. 5 Metal and metal oxide nanoparticle based hybrid nanofibers for anti-bacterial application. (a) Silver-doped polyurethane zein hybrid nanofibrous scaffold (AgNPs/PU-zein); (b) the water contact angle of AgNPs/PU-zein; (c) SEM image of the cell-cultured AgNPs/PU-zein scaffold for 7 days; the antibacterial activity of samples in against (d) *S. aureus* and (e) *E. coli*, respectively; reproduced with permission.[91] Copyright 2016, Elsevier. (f) Transmission electron microscope (TEM) image of PLGA/CuO hybrid nanofiber; (g) image of the inhibition zones of different nanofiber scaffolds against *E. coli* and *S. aureus*; (h) schematic diagram of the antibacterial mechanism of nano CuO/Cu^{2+} ions; reproduced with permission,[92] CC BY 4.0. (i) Schematic diagram of the antibacterial mechanism of electrospun PCL/ZnONPs; (j) the bacterial cell viability (%) of *S. aureus* in the different mats; reproduced with permission.[93] Copyright 2018, Elsevier. (k) Co-electrospun gelatin:TiO_2/PCL:silk fibroin scaffolds (G:T/P:F) for antisepsis; (l) the antibacterial activity of G/P:F and G:T/P:F scaffolds against *S. aureus* and *E. coli*. Reproduced with permission.[94] Copyright 2022, Wiley Periodicals LLC.

significant impediment to the healing process. Repeat infections not only retard the wound recovery but also pose considerable risks to individuals. Therefore, preventing bacterial intrusion into wounds is of paramount importance. Previous studies have demonstrated that certain inorganic nanoparticles possess broad-spectrum antibacterial properties and could circumvent bacterial drug resistance. Incorporating these anti-bacterial inorganic nanoparticles into polymer fibers proves to be an effective strategy for avoiding infections during the wound healing process.[87]

4.2.1. Metal nanoparticle based HNFs. A variety of metal nanoparticles have exhibited excellent antimicrobial activity in the context of wound healing. Silver nanoparticles (AgNPs), in particular, stand out as one of the most prominent antibacterial materials.[88–90] The Ag^+ released from AgNPs has been proven to hinder the growth of bacteria by adhering easily to the bacterial cell wall through hydrogen bonding and electrostatic forces.[88] Maharjan *et al.*[91] synthesized AgNPs by reducing a silver nitrate solution and utilized them to create silver-doped polyurethane zein (PU-zein) hybrid nanofibrous scaffolds by electrospinning (Fig. 5a). These PU-zein membranes, infused with AgNPs, exhibited excellent surface wettability, promoted cell proliferation and migration compared with pure PU (Fig. 5b and c). Moreover, they also showed significant inhibitory effects on both Gram-positive (*S. aureus*) and Gram-negative (*E. coli*) bacterial strains (Fig. 5d and e). Copper[95,96] and gold[37] nanoparticles embedded in polymer nanofibers have also demonstrated potent antibacterial activity in wound healing.

4.2.2. Metal oxide nanoparticle based HNFs. Several metal oxides hold great promise in hybrid nanofibers due to their satisfactory antimicrobial properties. For example, Haider *et al.*[92] developed wound healing solutions using copper oxide (CuO)-doped electrospun poly(lactide-*co*-glycolide)(PLGA) nanofibrous membranes (Fig. 5f). PLGA, on its own, has limited bactericidal abilities, but PLGA/CuO hybrid nanofibrous membranes displayed inhibitory zones against *E. coli* and *S. aureus*,

as observed through disc diffusion experiments (Fig. 5g). The inhibitory effect results from CuO/Cu^{2+} binding with sulfur-containing proteins in bacterial cell walls, impairing their function and eventually leading to bacterial cell death. Additionally, CuO or Cu^{2+} generates reactive oxygen species (ROS), inhibiting bacterial growth (Fig. 5h). Zinc oxide nanoparticles (ZnONPs) hinder bacterial growth by causing mechanical damage to bacterial cell membranes.[93,97,98] Velasquillo and coworkers [93]prepared polycaprolactone (PCL)/ZnONPs nanofibers through coaxial electrospinning.

These nanofibers facilitated the controlled release of Zn^{2+} and displayed enhanced antibacterial properties under UVA light irradiation (Fig. 5i), significantly reducing bacterial activity against *E. coli* and *S. aureus* (Fig. 5j) to about 20% after 72 hours when compared to pure PCL. Titanium dioxide nanoparticles (TiO_2NPs) can trigger antibacterial activity under ultraviolet irradiation. This effect is adjustable by manipulating parameters such as wavelength, light intensity, pH value, and temperature.[100,101] Consequently, TiO_2NPs find extensive application in wound treatment.[94,102–106] Recently, Golipour *et al.*[94] developed wound healing dressings by co-electrospinning of gelatin:TiO_2 and polycaprolactone:silk fibroin (G:T/P:F) (Fig. 5k). These scaffolds exhibited pronounced antibacterial activity against *E. coli* and *S. aureus* (Fig. 5l). Furthermore, the possible bacterial inhibitory mechanisms of TiO_2NPs were suggested: (i) TiO_2 leads to the peroxidation of polyunsaturated phospholipids in cell membranes and the loss of bacterial respiratory activity; (ii) the electrostatic interaction between TiO_2 and cell wall causes damage to the latter; (iii) TiO_2 generates ROS in body fluid environment, resulting in bacterial oxidative stress, thus destroying bacterial cells.

4.2.3. Inorganic nonmetallic nanoparticle based HNFs. Certain inorganic non-metallic nanoparticles boast exceptional antibacterial properties, making them valuable for wound healing applications. Graphene oxide (GO) is one of the most widely used carbon-based antibacterial materials due to its fruitful functional groups and strong biocompatibility.[99,107] Wang *et al.*[99] prepared graphene oxide nanosheets using the modified Hummers' method, and then combine them with silk protein (SF) through electrospinning to create SF/GO nanofibers (Fig. 6a). The findings of the study revealed that the survival rates of *E. coli* and *S. aureus* on SF nanofibers was (83.9 ± 7.0)% and (89.3 ± 4.8)%, respectively. In contrast, the survival rates of *E. coli* and *S. aureus* on SF/GO hybrid nanofibers were (35.7 ± 3.6)% and (41.6 ± 0.3)%, respectively (Fig. 6b). These results underscore the enhancement of antibacterial activity attributed to GO within the SF nanofiber matrix. Regarding the antibacterial mechanism of GO, it is widely accepted that GO disrupts the bacterial cell membrane, leading to the release of intracellular substances. This phenomenon is substantiated by the SEM images depicted in Fig. 6c, where *E. coli* displayed signs of atrophy and even membrane rupture upon contact with the SF/GO hybrid nanofibers.

Metal–organic frameworks (MOFs) have also attracted extensive attention as antibacterial materials in recent years because of their designability of molecular structure and controllability of releasing metal ions. The fine-tuning of antibacterial performance at the molecular level is achievable by regulating the metal ions and organic ligands within MOFs.[70,108–110] Most of the antimicrobial strategies of MOFs are mainly derived from two aspects: MOFs are reservoirs and sustained-release agents of antimicrobial metal ions or MOFs as porous materials are carriers of antimicrobial drugs. For example, as shown in Fig. 6d, Ning and colleagues[70] synthesized a silver(I) based metal organic framework (Ag_2[HBTC][IM], abbreviated as Ag-MOF). In their work, this Ag-MOF achieved high antimicrobial efficiency by slowly releasing silver ions. The Ag-MOF was uniformly mixed with PLA/DCM solution and subsequently electrospinning to form a Ag-MOF/PLA hybrid nanofiber membrane (Fig. 6e). Based on their results, Ag-MOF/PLA hybrid nanofibers presented potent inhibitory effects against *E. coli*, *P. aeruginosa*, *S. aureus*, and *M. smegmatis* (Fig. 6f). In contrast, both pure PLA and blank control group displayed negligible antibacterial activity, as is evident in Fig. 6g and h. However, the inhibition rates against *E. coli* and *S. aureus* of Ag-MOF/PLA with a concentration of 2.5 wt% Ag-MOF reached 97.2%, and 97.5%, respectively.

4.2.4. Other inorganic nanoparticle based HNFs. In addition to the commonly used HNFs mentioned in the previous sections, other inorganic materials such as cerium (Ce),[111] iodine(I),[112] and selenium (Se)[113] have been developed for doping of polymer nanofibers, exhibiting notable antimicrobial activity.

We have summarized the HNFs with antibacterial activity and other functions in Table 1.

4.3. Cell proliferation and migration

Proliferation and migration of the fibroblasts, endothelial cells, and keratinocytes allow the establishment of a new extracellular matrix and granulation tissue, which are essential for wound closure.[122] Inorganic nanoparticles, including metals (Ag[123]) and metal oxides (ZnO,[124] and Fe_2O_3[125]) as well as inorganic nonmetallic materials (Si,[56,126] GO,[99] and MOF[109]) have demonstrated the ability to promote cell proliferation and migration. In addition to the above, some materials have been considered for their versatility to promote cell proliferation and migration in wound therapy, such as cuprous sulfide (CuS), cerium oxide (CeO_2) and biological glass (BG).

4.3.1. Metal sulfide nanoparticle based HNFs. Metal sulfide materials, such as cuprous sulfide (Cu_2S), exhibit exceptional photothermal effects. Beyond their application in treating skin defects caused by tumors, these materials hold great potential in wound healing procedures. Wu and colleagues[127] synthesized Cu_2S (CS) nanoparticles by using a hydrothermal method and incorporated them into a mixed solution of poly(lactic acid)/polycaprolactone (PLA/PCL) to prepare electrospun hybrid nanofibers. The resulting CS-PLA/PCL membranes were assessed for their impact on cell proliferation and migration (Fig. 7a). Briefly, human dermal fibroblasts (HDFs) and human umbilical vein endothelial cells (HUVECs) were cultured on the as-prepared nanofibrous membranes without Cu_2S (0CS) and with 30 wt% of Cu_2S (30CS). The cell

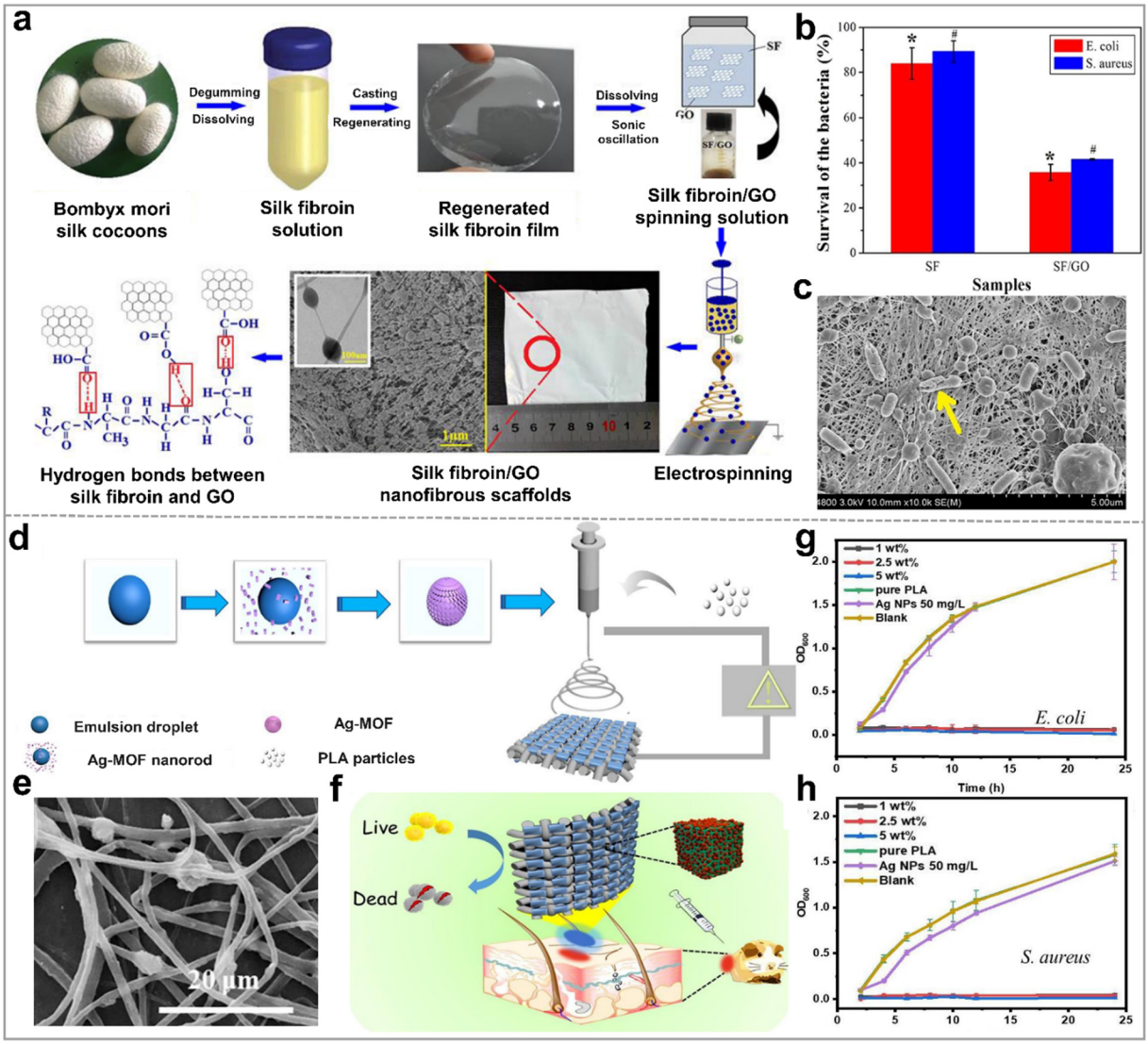

Fig. 6 Anti-bacterial ability of inorganic nonmetallic nanoparticle based hybrid nanofibers. (a) Schematic illustration of the preparation process of silk fibroin/GO nanofibrous scaffolds(SF/GO); (b) survival rates of bacteria (%) on the nanofibers (c) SEM image of *E. coli* on the surface of SF/GO-blended nanofibers; reproduced with permission,[99] CC BY 4.0. (d) Schematic diagram of the preparation process of the electrospun fibrous mat based on silver(I)-MOF/poly(lactic acid) (Ag-MOF/PLA) for bacterial killing; (e) SEM image of Ag-MOF/PLA; (f) schematic diagram of the antibacterial applications of Ag-MOF/PLA; growth activity of (g) *E. coli* and (h) *S. aureus* on Ag-MOF/PLA, pure PLA, and commercial AgNPs; reproduced with permission.[70] Copyright 2020, Elsevier.

counting kit-8 (CCK-8) assay revealed that HDFs cultured on the hybrid nanofiber membrane exhibited a higher proliferation rate than the control group (Fig. 7b). Additionally, the *in vitro* scratch test of HUVECs demonstrated that the scratch of the 30CS-PLA/PCL group almost disappeared after 6 hours, as shown in Fig. 7c. Compared to the control group (28.1%) and the 0CS-PLA/PCL group (18.4%), the relative wound area of the 30CS-PLA/PCL group was mere 5.1% (Fig. 7d). These results underscored that the addition of Cu_2S nanoparticles improved the regeneration activity of the nanofibrous membrane *in vitro* and promoted the proliferation and migration of the cells in the wound area.

4.3.2. Metal oxide nanoparticle based HNFs. Numerous metal oxide nanoparticles have been reported as effective materials to improve cell proliferation and migration for the wound healing process. For instance, cerium oxide nanoparticles (CeNPs), known for their antioxidant and regenerative properties, hold great promise in the biomedical field.[111,128] As depicted in Fig. 7e, Lv *et al.*[128] prepared CeNPs doped poly(L-lactic acid)–gelatin (PLLA–gelatin) nanofibers through direct electrospinning for wound healing. Results from acridine orange/ethidium bromide (AO/EB) staining indicated that the cell densities of NIH 3T3 in the PLLA–gelatin membrane doped with 0.25 w%(C2-M) and 0.5 w%(C2-H) CeNPs were significantly higher than those in the PLLA–gelatin membrane and pure PLLA membrane (Fig. 7f). Moreover, CCK-8 assay results indicated that the viability of L929 cells in the C2-H group exceeded that in the other groups (Fig. 7g). Therefore, it was

Table 1 Electrospun organic/inorganic hybrid nanofibers (HNFs) used as anti-bacterials

Inorganic components	Polymers	Methods of incorporation	Functions	Ref.
AgNPs	Polyurethane	Electrospinning with subsequent loading	Antibacterial activity against *E. coli* and *S. aureus*, and promotion of cell proliferation	91
	Polyvinyl alcohol/chitosan	Direct electrospinning	Antibacterial activity against *E. coli* and *S. aureus*	114
	Polycaprolactone	Direct electrospinning	Antibacterial activity against *E. coli* and *S. aureus*, and promoting cell attachment, proliferation and spreading	89
	Thermoplastic polyurethane, polyvinyl alcohol	Electrospinning with subsequent loading	Antibacterial activity against *E. coli*, *S. aureus*, MRSA, Acinetobacter, and Klebsiella-pneumoniae	88
	Polycaprolactone/polyvinyl pyrrolidone	Direct electrospinning	Antibacterial activity against *E. coli* and *S. aureus*	115
	Silk fibroin	Direct electrospinning	Antibacterial activity against *S. aureus*, *S. epidermidis*, and *P. aeruginosa*	116
	Polyethylene oxide/carboxymethyl chitosan	Direct electrospinning	Antibacterial activity against *P. aeruginosa*, *E. coli*, and *S. aureus*	117
	Polyvinyl alcohol/chitosan	Electrospinning with subsequent loading	Antibacterial activity against *E. coli*	118
Cu, CuONPs	Poly(lactide-*co*-glycolide)	Direct electrospinning	Antibacterial activity against *E. coli* and *S. aureus*, and promotion of cell adhesion, proliferation and viability	92
	Polyvinyl pyrrolidone	Direct electrospinning	Antibacterial activity against *E. coli*, *P. aeruginosa*, *S. aureus* and *Bacillus cereus*	95
	Polycaprolactone/gelatin	Direct electrospinning	Antibacterial activity against *E. coli* and *S. aureus*	96
ZnONPs	Polyacrylic acid/polyallylamine hydrochloride	Electrospinning with subsequent loading	Antibacterial activity against *E. coli* and S. aureus	97
	Polycaprolactone	Coaxial electrospinning	Antibacterial activity against *E. coli* and *S. aureus*	93
	Chitosan/polycaprolactone	Direct electrospinning	Antibacterial activity against *S. aureus* and *B. subtilis*, antioxidant activity and ability to accelerate wound healing	98
	Vinylidene fluoride-tetrafluoroethylene copolymer/polyvinyl pyrrolidone	Direct electrospinning	Antibacterial activity against *S. aureus*, and positive contribution to purulent wound healing	119
TiO_2NPs	Polycaprolactone	Direct electrospinning	Antibacterial activity against *E. coli* and *S. aureus*, and promotion of cell adhesion and viability	100
	Polyurethane	Electrospinning with subsequent loading	Antibacterial activity against *S. aureus* and *P. aeruginosa*, and good cell adhesion	105
	Chitosan/pectin	Direct electrospinning	Antibacterial activity against *E. coli*, *S. aureus*, *P. aeruginosa*, absorption of wound exudate and acceleration of wound closure	102
	Silk fibroin	Direct electrospinning	Antibacterial activity against *E. coli*, and promotion of cell adhesion and growth	104
	Chitosan/polyvinyl pyrrolidone	Direct electrospinning	Antibacterial activity against *E. coli*, *S. aureus*, *P. aeruginosa*, and *B. subtilis*, and *B. subtilis*, and promotion of wound closure	106
	Gelatin/polycaprolactone/silk fibroin	Direct electrospinning	Antibacterial activity against *E. coli* and *S. aureus*, and acceleration of cell proliferation and migration	94
	Polylactic acid	Direct electrospinning	Antibacterial activity against *S. aureus*	101
	Chitosan	Direct electrospinning	Antibacterial activity against *S. aureus*	120
Iodine	Polyvinyl pyrrolidone/polyvinyl butyral	Direct electrospinning	Antibacterial activity against *E. coli* and *S. aureus*	112
GO	Silk fibroin	Direct electrospinning	Antibacterial activity against *E. coli* and *S. aureus*, and acceleration of cell proliferation and migration	99
MOFs	Polylactic acid	Direct electrospinning	Antibacterial activity against *E. coli*, *P. aeruginosa*, *S. aureus*, and *M. smegmatis*, and acceleration of wound healing	70
	Chitosan/polyvinyl alcohol	Direct electrospinning	Antibacterial activity against *E. coli* and *S. aureus*	108
CeO_2/bioglass	Chitosan/polyethylene oxide	Direct electrospinning	Antibacterial activity against *E. coli* and *S. aureus*	111
SeNPs	Polycaprolactone/gelatin	Direct electrospinning	Antibacterial activity against *S. aureus* and *P. aeruginosa*, and promotion of wound closure	121

concluded that CeNPs hybrid nanofibers substantially promoted the proliferation of cells.

4.3.3. Bioglass-based HNFs. Bioglass (BG), an artificial inorganic material rich in bioactive oxides, has attracted considerable

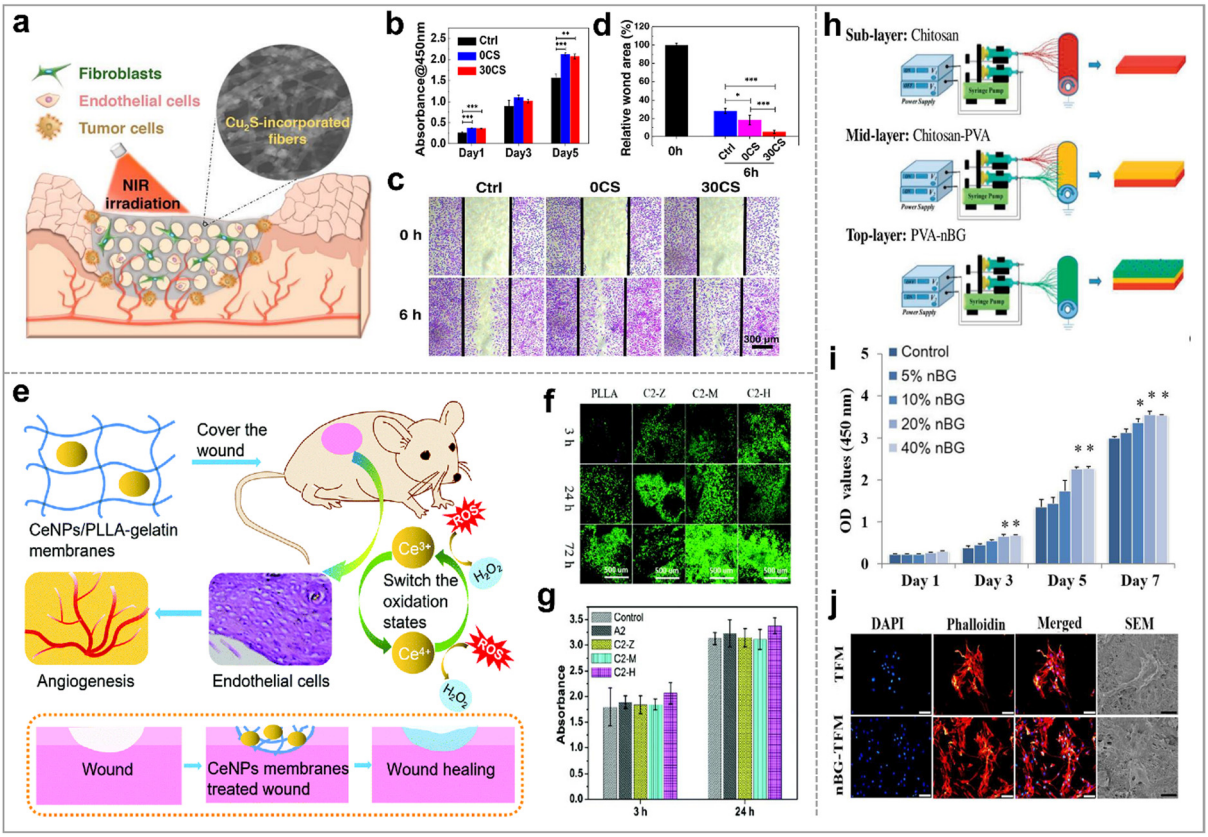

Fig. 7 Bioglass-based hybrid nanofibers for promoting cell proliferation and migration. (a) Electrospun nanocomposites incorporated with Cu_2S nanoflowers for skin tumor therapy and wound healing; (b) the cell proliferation of HDFs cultured on the different membranes for 1, 3, 5 days; (c) *in vitro* scratch assay of HUVECs on the various membranes. (d) The relative wound area; reproduced with permission.[127] Copyright 2017, American Chemical Society. (e) Schematic illustration of the mechanism of CeNPs/PLLA–gelatin for wound healing *via* generation of ROS, proliferation and migration of the endothelial cells, and angiogenesis; (f) distribution and density of NIH 3T3 cells (AO/EB staining), and (g) cell activity of L929 cells (CCK-8 assay) on the various nanofiber membranes; reproduced with permission.[128] Copyright 2022, Royal Society of Chemistry. (h) Schematic diagram of the preparation of the nano bioglass/three-layer composite nanofibrous membrane (nBG–TFM); (i) proliferation of L929 cells on nBG–TFM; (j) morphology of HDF cells on the nBG–TFM and non-nBG (TFM); reproduced with permission.[129] Copyright 2019, Elsevier.

attention for its excellent wound healing properties.[111,129,130] Chen *et al.*[129] prepared nano-bioglass (nBG) by the sol–gel method. Subsequently, they fabricated a three-layer composite nanofibrous membrane (nBG–TFM) with chitosan and poly(vinyl alcohol) (PVA) using the sequential electrospinning technique (Fig. 7h). L929 cells was cultured on nBG–TFM with varying nBG concentrations to investigate its effects on cell proliferation. As shown in Fig. 7i, the number of cells increased with higher content of nBG content. HDFs exhibited elongated cytoskeletons and increased filopodia abundance when cultured on a membrane containing 40% nBG (Fig. 7j). This can be attributed to the presence of TFM and nBG, which elevated basic fibroblast growth factor (bFGF) levels and promoted type I collagen deposition, ultimately stimulating cell proliferation and migration.

4.4. Angiogenesis

Blood vessels play a crucial role in facilitating the exchange of substances between the blood and tissue, providing essential nutrients for cell growth. Therefore, angiogenesis, the formation of new blood vessels, is a pivotal step in wound healing. Growth factors such as the vascular endothelial growth factor (VEGF), epidermal growth factor (EGF), stromal cell-derived factor (SDF) have been proven effective in accelerating wound revascularization. However, medical products based on growth factor face limitations such as short release time and high cost.[58,131,133] Thus, researchers are searching satisfactory organic/inorganic hybrid materials to accelerate angiogenesis.

4.4.1. Bioglass-based HNFs. Bioglass/bioceramics have emerged as bioactive nanoparticles with potential to promote wound angiogenesis.[58,129,131] As depicted in Fig. 8a, a hybrid nanofiber consisting of bioglass (BG) and patterned electrospun membrane (PEM) nanofibers were prepared by initially electrospinning poly(DL-lactic acid) (PDLLA) nanofibers with subsequent loading BG *via* pulsed laser deposition technology. The performance of as-prepared hybrid nanofibers was evaluated using a rat wound model (Fig. 8b).[131] Digital images of the wound angiogenisis on the 15th day showed that BG/PEM hybrid nanofibrous membrane increased the number of blood vessels compared to the control group and the PEM group (Fig. 8c). Quantitative analysis of the wound neovascularization also confirmed that the BG/PEM group exhibited the highest capillary density and the best vascular regeneration

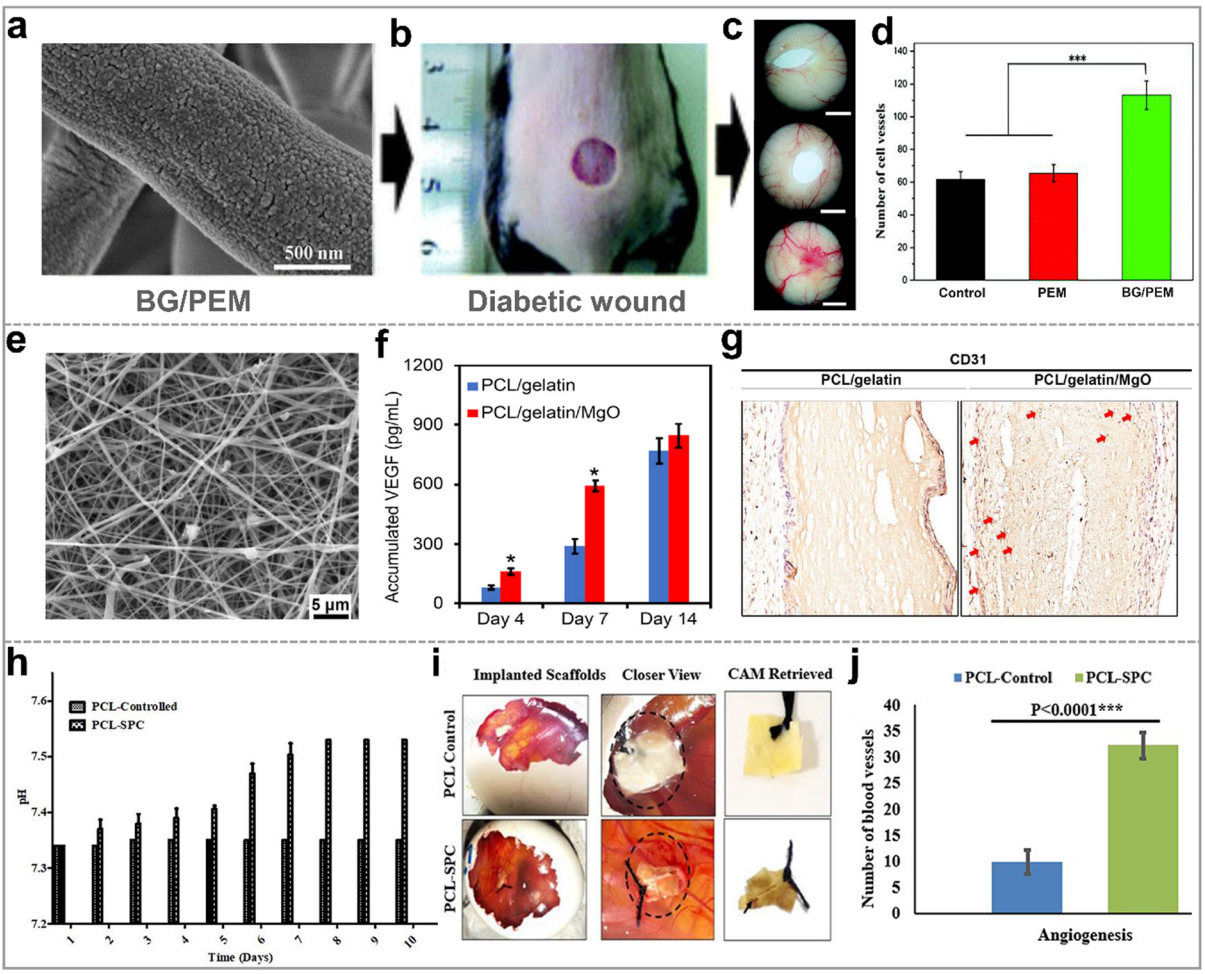

Fig. 8 Hybrid nanofibers for promoting blood vessel generation. (a) SEM image of BG/PEM; (b) BG/PEM used for the diabetic wound treatment and (c) digital image of new blood vessels for 15 days; (d) statistical analyses of the number of new blood vessels; reproduced with permission.[131] Copyright 2017, Royal Society of Chemistry. (e) SEM image of PCL/Gelatin/MgO; (f) PCL/Gelatin/MgO produced more VEGF than PCL/Gelatin; (g) immunohistochemical staining of subcutaneously implanted electrospun membranes for 14 days; reproduced with permission.[132] Copyright 2021, Elsevier. (h) Evaluation of the oxygen release of the electrospun PCL–SPC nanofibers over 10 days; (i) digital images of the new blood vessels in chorioallantoic membrance (CAM) assay; (j) quantification of the blood vessels using different scaffolds; originally published by and used with permission from Dove Medical Press Ltd.[61]

effect (Fig. 8d). This promotion can be attributed to the release of silicon ions and calcium ions from BG, which stimulated the growth of the fibroblasts and endothelial cells and enhanced the expression of angiogenesis-related growth factors (VEGF, bFGF, *etc.*).

4.4.2. Metal nanoparticle based HNFs. Magnesium (Mg) is commonly adopted to accelerate blood vessel regeneration. It has been evidenced that a low concentration of Mg can enhance cell migration and the expression of vascular-related genes, such as HIF-1α and VEGF, to stimulate angiogenesis.[134,135] Wu and coworkers[132] prepared MgO-doped PCL/Gelatin electrospinning nanofibers to improve angiogenic activity and diabetic wound healing (Fig. 8e). As shown in Fig. 8f, endothelial cells stimulated by PCL/Gelatin/MgO exhibited twice as much VEGF secretion compared to those on PCL/Gelatin. Furthermore, after implanting these electrospun membranes under the skin, negligible newly formed blood vessels were observed on wounds with PCL/Gelatin as dressing after 14 days, while numerous newly formed capillaries were evident on wounds with PCL/Gelatin/MgO as dressing (Fig. 8g).

4.4.3. Oxygen releasing materials based HNFs. Appropriate amount of oxygen will enhance the wounds angiogenesis and accelerate the healing process. Oxygen releasing materials (ORMs), represented by sodium percarbonate (SPC), calcium peroxide (CPO), magnesium peroxide (MPO), and hydrogen peroxide (HPO), have become a key focus in wound repair.[60,61,136] Sodium percarbonate (SPC), an oxygen-producing compound that reacts with water to form H_2O_2 and Na_2CO_3, was blended with PCL in DCM and DMF, resulting in the preparation of PCL–SPC hybrid nanofibrous membranes *via* electrospinning.[61] In this study, the released amount of oxygen was reflected by the increase of pH value. The decomposition of SPC produced carbonate, which was further hydrolyzed to generate OH-ions, lead to

an elevated pH value. As exhibited in Fig. 8h, the pH value of the PCL–SPC group increased uniformly, while the pH of the pure PCL group remained constant. Thus, the PCL–SPC group released oxygen during the experiment. The chorioallantoic membrane (CAM) assay revealed a larger number of blood vessels in the PCL–SPC group compared to the pure PCL control group (Fig. 8i), and the quantitative blood vessel counting confirmed that a certain amount of oxygen promoted angiogenesis (Fig. 8j).

4.5. Other direct applications

4.5.1. Anti-inflammatory. Strategies that can regulate the innate immune cells (especially macrophages) and cytokines to fight inflammation have gained increasing attention.[58,137,138] Before transitioning to the cell proliferation and migration stages, wounds undergo an inflammatory phase where invading microorganisms are engulfed and eliminated. However, chronic wounds often result in a persistent inflammatory state,

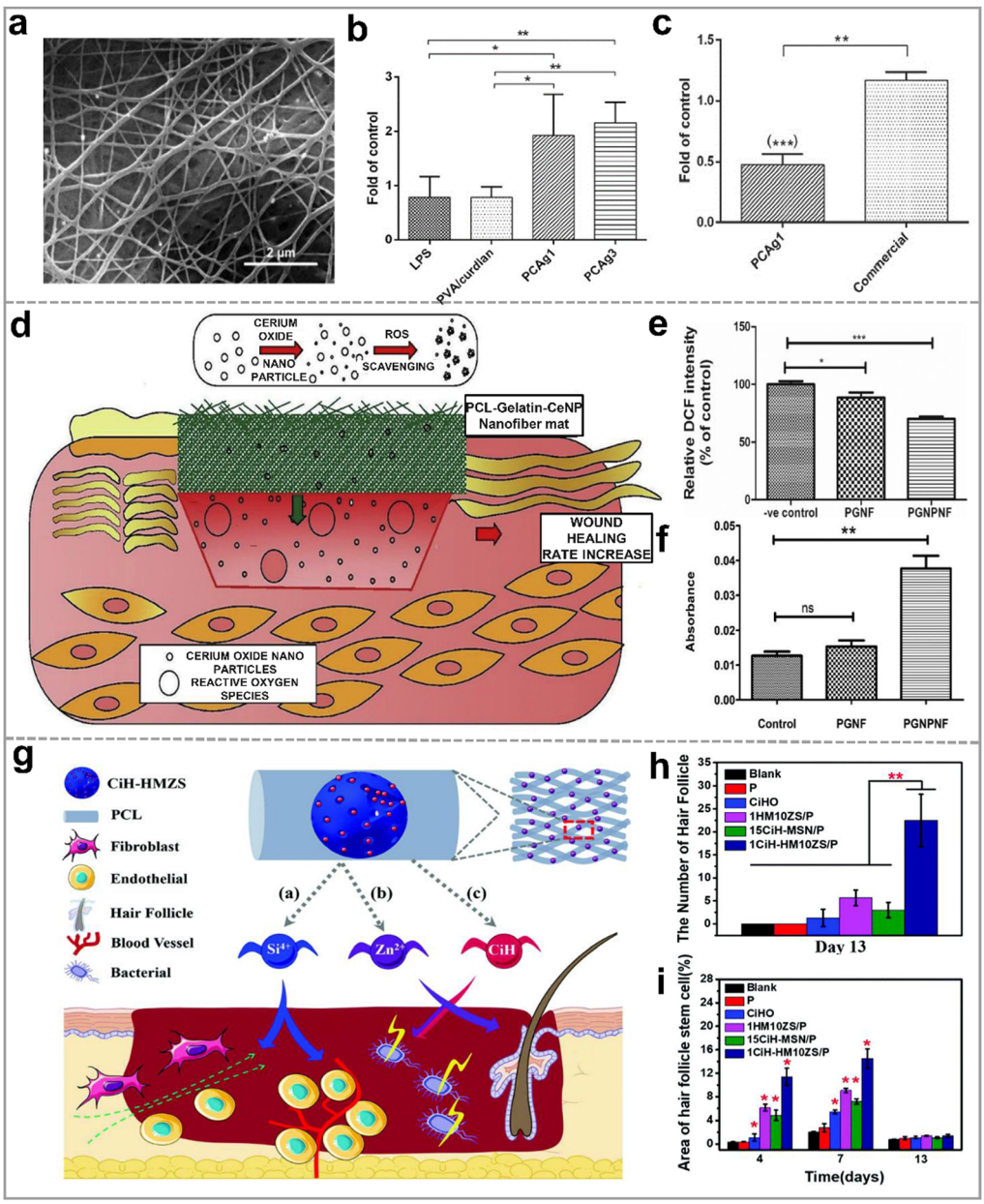

Fig. 9 (a) SEM image of PVA/curdlan nanofibers with 1% $AgNO_3$ (PCAg1); (b) *in vitro* mRNA expression levels of TGFβ1 inflammatory cytokines in the mouse macrophages with the different nanofibrous mats; (c) effect of PCAg1 on mRNA expression levels of IL1β on day 14; reproduced with permission.[141] Copyright 2018 Wiley-VCH Verlag GmbH & Co. KGaA, Weinheim. (d) Schematic illustration of the antioxidant mechanism of CeNPs functionalized PCL-Gelatin nanofibers; (e) ROS level measurement in 3T3-L1 cells on various nanofibers by the DCF fluorescence intensity; (f) the cell viability of 3T3 L1 on different nanofibers against the ROS measurement by the alamar blue assay; reproduced with permission,[142] CC BY-NC-ND 4.0. (g) Schematic diagram of zinc-loaded hollow mesoporous silica/PCL electrospun nanofibers promoting hair follicle regeneration; (h) quantification of the new hair follicles for 13 days; (i) quantification of the area of hair follicle stem cell on day 4, 7, and 13; reproduced with permission.[124] Copyright 2019, Royal Society of Chemistry.

severely impeding the healing process. Therefore, it is reasonable to perform immune regulation at the wound site to accelerate the transition from inflammation to proliferation.[139,140] Rubaiya *et al.*[141] prepared poly(vinyl alcohol) (PVA)/curdlan electrospun nanofibrous scaffolds (PCAg) loaded with AgNPs to mitigate wound inflammation (Fig. 9a). The results demonstrated a reduction in the expression level of the proinflammatory cytokine Interleukin-6 (IL6), a representative indicator of inflammation, in response to the low concentration of silver-loaded nanofibrous scaffolds (PCAg1) (Fig. 9b). Simultaneously, the expression of anti-inflammatory cytokine Transforming Growth Factor β1 (TGFβ1) increased, indicating that the PCAg1 scaffold effectively mitigated inflammation by modulating IL6 and TGFβ1 (Fig. 9c).

4.5.2. Antioxidation. Reactive oxygen species (ROS) play a pivotal role in the wound healing process. An appropriate level of ROS can inhibit the growth of bacteria[93,143] while promoting tissue re-epithelialization and vascular regeneration.[142,144,145] However, excessive ROS has the adverse effects on the protein, DNA, and other macromolecules, leading to inflammation, cell senescence, and fibrotic scarring.[142,146,147] Therefore, wound dressings designed to maintain proper ROS levels will facilitate the wound healing procedure. Rather *et al.*[142] fabricated cerium nanoparticles (CeNPs) functionalized PCL–gelatin nanofibrous (PGNPNF) membranes for antioxidant therapy in wound healing (Fig. 9d). According to the *in vitro* antioxidant experiment, the intensity of the 2′,7′-dichlorofluorescein (DCF, a fluorescent compound formed by oxidation of ROS) fluorescence intensity of the cells treated with the nanofibrous membrane (PGNF) without CeNPs decreased by 12% while the DCF fluorescence intensity of the cells treated with PGNPNF decreased by 30%, compared with the control group, indicating that PGNPNF could remove ROS (Fig. 9e). In addition, after treating PGNPNF with H_2O_2 for 24 h, it was observed that the cells in the PGNPNF group had strong antioxidant activity and ROS scavenging ability, which increased the cell viability by approximately threefold compared with the control group (Fig. 9f). These results

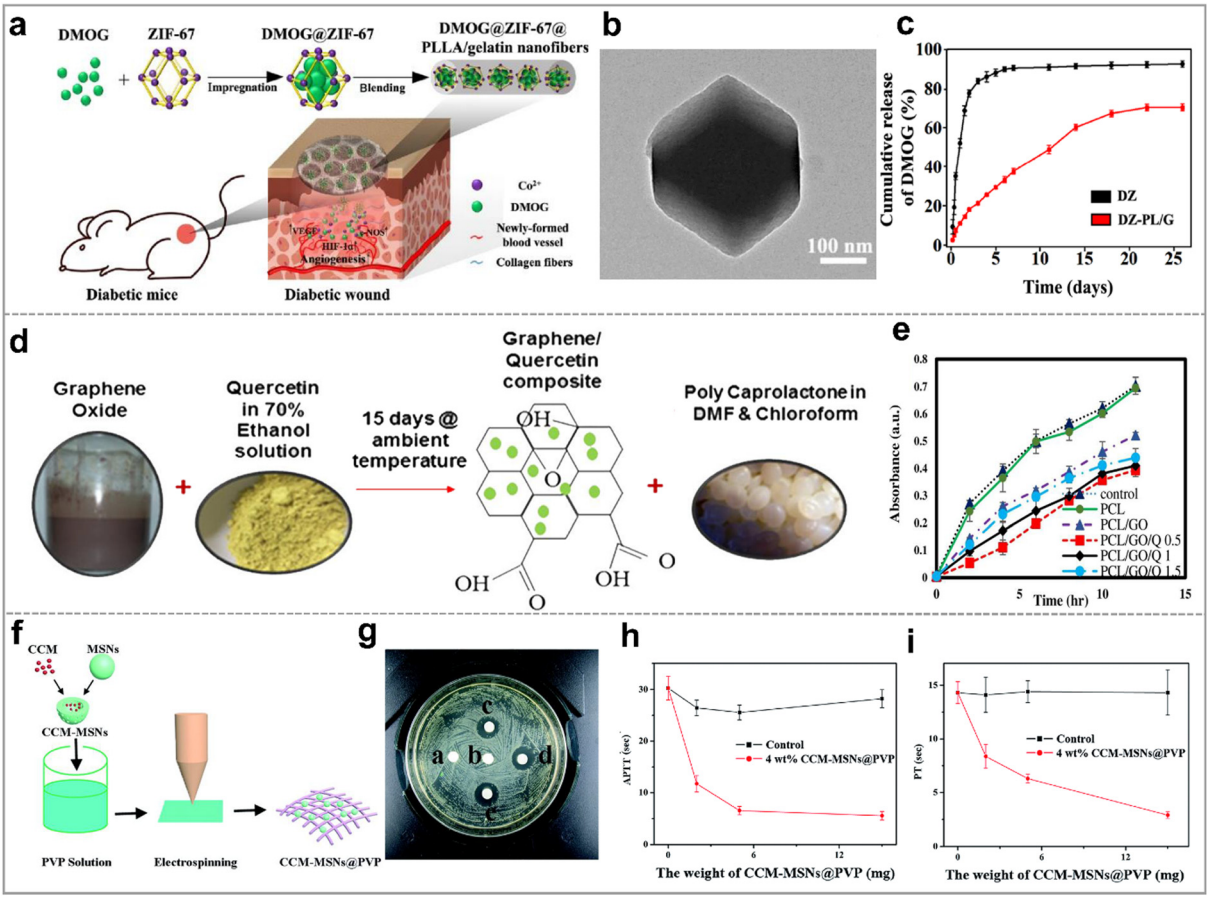

Fig. 10 Hybrid nanofibers as drug carriers for promoting wound healing. (a) Schematic illustration of PCL/gelatin nanofibers with ZIF-67 that loading DMOG for wound healing; (b) TEM image of ZIF-67; (c) the release profiles of DMOG from (ZIF-67)DZ and (ZIF-67-PLLA/gelatin)DZ-PL/G; reproduced with permission.[148] Copyright 2020, Tsinghua University Press and Springer-Verlag GmbH Germany, part of Springer Nature. (d) Schematic diagram of electrospun PCL/GO/quercetin nanofibrous scaffolds; (e) antibacterial activities of PCL nanofibrous scaffolds with the varying contents of GO and quercetin against *S. aureus*; reproduced with permission.[149] Copyright 2020, Elsevier. (f) Schematic illustration of the preparation process of CCM-MSNs@PVP nanofiber mats; (g) image of the inhibition zones of the different mats against MRSA strain for 48 h, (a)–(e) represent pure PVP, 4 wt% MSNs@PVP nanofiber mats, 2 wt% MSNs@PVP nanofiber mats, 4 wt% CCM-MSNs@PVP nanofiber mats, and 8 wt% CCM-MSNs@PVP nanofiber mats, respectively; results of (h) APTT and (i) PT tests of CCM-MSNs@PVP nanofiber mats; reproduced with permission.[150] Copyright 2017, Royal Society of Chemistry.

indicated that CeNP hybrid nanofibers possessed antioxidant activities and could effectively scavenge ROS.

4.5.3. Hair follicle regeneration. Effective wound healing not only ensures wound closure but also involves the regeneration of hair follicles, sweat and sebaceous glands, and other skin appendages to fully recover the structural and functional integrity of the skin.[16,59,151] Zinc is an important cofactor for numerous enzymes, including those with crucial roles in hair follicles. In recent years, zinc-contained drugs have been employed for the treatment of hair-related diseases. To develop an organic/inorganic hybrid nanofiber membrane with hair follicle regeneration activity, Chang and colleagues[124] prepared Zn-doped hollow mesoporous silica nanospheres (HMZS) by the sol–gel method. A hybrid nanofibrous membrane (HM10ZS/P) was subsequently obtained by electrospinning pre-mixed HMZS/PCL materials for hair follicle regeneration (Fig. 9g). Based on the number of hair follicles (Fig. 9h) and the area of hair follicle cells (Fig. 9i), the PCL nanofibrous membrane (1HM10ZS/P) loaded with a 1% concentration of HM10ZS was outperformed the control group and pure PCL membrane (P) group.

4.6. Drug loading

While the premixed drug/polymer followed by electrospinning method is simple and convenient, it falls short in achieving controlled and sustained drug release, limiting its potential in accelerating wound healing. This can be suitably resolved by using integrated nanofiber membrane/porous inorganic as drug carriers. Consequently, a wide array of drugs, including hemostatic agents, antibacterial agents, antioxidants, and many other drugs are encapsulated in these materials for wound treatment.

4.6.1. MOF-based HNFs. Metal–organic frameworks (MOFs) are crystalline materials known for their high porosity and molecular-level controllability. This characteristic enables synergistic interactions with drugs.[152] As shown in Fig. 10a, Li *et al.*[148] loaded the angiogenic small molecule drug, dimethoxyglycine (DMOG), onto the cobalt-based ZIF-67 (DZ, morphology is shown in Fig. 10b). This composite was subsequently electrospun with the PLLA/gelatin to create the hybrid nanofibrous material DZ-PL/G. During *in vitro* DMOG release tests, DZ-PL/G showed a stable release rate compared to the DZ group, demonstrating effective control over DMOG release through diffusion and degradation of the hybrid nanofiber membrane (Fig. 10c). Researchers have also loaded MOFs with tannic acid,[153] curcumin,[54] and other drugs, highlighting the great potential of MOF/electrospun nanofiber membranes in drug delivery.

4.6.2. Graphene oxide based HNFs. Graphene oxide (GO), a sheet-like carbon-based material, has gained significant attention in wound treatment due to its excellent mechanical properties, large specific surface area, good chemical stability, and low toxicity.[39,113,149,154] Faraji *et al.*[149] incorporated quercetin (Q) and GO nanosheets to PCL and then fabricated the nanofibrous membranes by electrospinning (Fig. 10d). Antibacterial results revealed a 25% reduction in *S. aureus* growth activity in the

Table 2 Electrospun organic/inorganic hybrid nanofibers (HNFs) used for the loading drugs

Inorganic carriers	Organic polymers	Drugs	Application	Ref.
ZIF-67	Polylactic acid	Dimethyloxalylglycine (DMOG)	Enhances angiogenesis, promotes collagen deposition, and eliminates inflammation	148
ZIF-8	Chitosan/polyvinyl alcohol	Tannic acid (TA)	Improves antibacterial activity and accelerates the aggregation of the coagulation factors and platelets	153
	Polycaprolactone	Rose Bengal (RB)	Improves antibacterial activity and accelerates wound healing	161
	Polylactic acid	Curcumin (CCM)	Inhibits inflammatory response and promotes collagen deposition, angiogenesis, and re-epithelialization	54
HKUST-1	Citrus pectin	Folic acid	Improves the mechanical strength and antibacterial activity, induces the angiogenesis, and promotes fibroblast migration and proliferation	162
	Polycaprolactone	Nitric oxide (NO)	Promotes endothelial cell growth and improves angiogenesis, collagen deposition, and anti-inflammatory property	163
GO	Polycaprolactone	Quercetin	Improves antibacterial activity	149
	Chitosan/polyvinyl alcohol	Ciprofloxacin	Improves antibacterial activity	154
	Polyethylene oxide	CeO_2 and peppermint oil	Improves antibacterial activity and accelerates re-epithelialization and collagen deposition	39
	Polylactic acid	Se/clarithromycin	Improves antibacterial activity	113
MSNs	Polyvinyl pyrrolidone	Curcumin (CCM)	Improves antibacterial activity and activates the clotting system to stop wound bleeding	150
	Poly(lactide-*co*-glycolide)	Andrographolide	Promotes epidermal cell adhesion and reduces inflammation process	155
	Polylactic acid	Levofloxacin (lev) and Ag	Inhibites bacterial growth and infection	156
	Polycaprolactone	Curcumin (CCM)	Improves antibacterial activity	157
	Polycaprolactone	Levofloxacin	Improves antibacterial activity	158
	Polycaprolactone	Methylene blue	Improves antibacterial activity	159

PCL/GO group compared to pure PCL nanofibers. Moreover, the growth activity of *S. aureus* in the PCL/GO/Q0.5 group reduced to 56% (Fig. 10e). It was concluded that PCL/GO hybrid nanofibrous loaded with quercetin exhibit significantly enhanced antibacterial activity against *S. aureus*.

4.6.3. Mesoporous silica based HNFs. Mesoporous silica (MSNs) is a cost-effective and common porous drug-loading material increasingly integrated into electrospun nanofibers as drug carriers for wound healing in recent years.[155–160] Li *et al.*[150] blended curcumin-loaded mesoporous silica nanoparticles (CCM-MSNs) with PVP and then employed electrospinning to produce hemostatic and antibacterial nanofibrous membranes (Fig. 10f). The diameter of the inhibition zone indicated that the hybrid nanofibers with higher CCM-MSN content had a stronger bacteriostatic effect (Fig. 10g). Whole blood absorption and coagulation tests revealed higher plasma absorption rates for CCM-MSN hybrid nanofibers. Additionally, they could activate both internal (Fig. 10h) and external (Fig. 10i) coagulation pathways, inducing coagulation and significantly shortening hemostasis time.

We have investigated and summarized some cases of electrospun nanofibers loaded with wound-healing drugs using MOF, GO or MSN in Table 2.

5. Conclusions and future perspectives

Electrospun organic/inorganic hybrid nanofibers are highly promising candidates for promoting wound healing due to the synergistic effect of electrospun nanofibers' ECM-mimicking architecture of and the biological activities in inorganic nanomaterials. This paper has delineated the several methods for crafting these hybrid nanofibers. Notably, premixing inorganic and organic constituents before electrospinning stands as the simplest and most prevalent technique, offering precise control over component ratios. While coaxial electrospinning introduces complexity, its paramount advantage lies in controlled release of inorganic ions or therapeutic agents. The approach of electrospinning with subsequent loading adeptly secures inorganic nanoparticles onto nanofiber surfaces, affording tailored morphologies conducive to regulating cell responses. However, unlocking the full potential of uniform nanoparticle distribution within polymer nanofibers mandates advanced electrospinning and synthetic methodologies. Furthermore, comprehensively investigating the bonding mechanisms underpinning interactions between inorganic nanoparticles and organic nanofibers is imperative, as it will further illuminate the design principles governing hybrid nanofiber fabrication.

The applications of electrospun organic/inorganic hybrid nanofibers in accelerating the various stages of wound healing, encompassing hemostasis, antibacterial, cell proliferation and migration, angiogenesis, *etc.* have been summarized. Briefly, clay mineral nanoparticle-based hybrid nanofibers emerge as preferable choices for hemostasis. Beyond frequently used metal-based nanomaterials (Ag, ZnO, CuO, TiO_2, *etc*), inorganic non-metallic nanomaterials (GO, MOF, *etc*) have demonstrated remarkable efficacy in thwarting bacterial infections. Bioglass has proven to be effective in promoting cell proliferation and migration, and even angiogenesis. Among the array of inorganic nanoparticles, ZnO stands as the most favored due to the antibacterial activity of Zn^{2+} ions and their capacity to stimulate blood vessel regeneration. Polymers like PLLA and PLGA are also commonly employed, owing to their biocompatibility and facile electrospinning characteristics. However, the biotoxicity of these inorganic nanoparticles and their circulation/expulsion pathways *in vivo* remain to be fully investigated. In other words, the concentration of each component in the hybrid nanofibers and controllable release of ions need to be delicately regulated to avoid potential side effects.

Looking ahead, a pivotal shift in the landscape of wound dressings foresees the emergence of bioabsorbable materials to alleviate the challenges associated with dressing changes. Consequently, there is an escalating demand for multifunctional organic/inorganic hybrid nanofibers engineered to accelerate all four stages of the wound healing process within a single dressing. Besides, multiple fluid electrospinning and the resultant multiple-chamber nanostructures that can tailor the ingredients and hierarchical structures of the hybrid nanofibers is a new direction worth developing. The biological mechanisms governing the efficacy of inorganic materials and the *in vivo* degradation products of biopolymers in promoting wound healing require further exploration. Innovative methodologies like high-throughput screening and organs-on-chips hold immense potential for expediting the development of novel hybrid nanofibers and reducing reliance on animal experimentation. Through collaborative endeavors among researchers from diverse domains including materials science, bioengineering, and clinical practice, electrospun organic/inorganic hybrid nanofibers are poised for a promising and commercially prosperous future.

Conflicts of interest

The authors declare no competing financial interest.

Acknowledgements

This work was supported by the National Key Research and Development Program of China (2021YFA1201304/2021YFA 1201300), the National Natural Science Foundation of China (52103298 and 52350410453), the Fundamental Research Funds for the Central Universities (2232022D-01), the Science and Technology Commission of Shanghai Municipality (20DZ2254900), and the Young Elite Scientists Sponsorship Program by CAST (YESS20220259). We thank Dr Xuechen Wu from Shanghai Starriver Bilingual School for language editing.

Notes and references

1 S. Homaeigohar and A. R. Boccaccini, *Acta Biomater.*, 2020, **107**, 25–49.
2 K. Chen, H. Hu, Y. Zeng, H. Pan, S. Wang, Y. Zhang, L. Shi, G. X. Tan, W. S. Pan and H. Liu, *Eur. Polym. J.*, 2022, **178**, 111490.
3 G. Rivero, M. Meuter, A. Pepe, M. G. Guevara, A. R. Boccaccini and G. A. Abraham, *Colloids Surf., A*, 2020, **587**, 124313.
4 E. J. Jang, R. Patel and M. Patel, *Pharmaceutics*, 2023, **15**, 1144.
5 L. Yang, D. Zhang, W. Li, H. Lin, C. Ding, Q. Liu, L. Wang, Z. Li, L. Mei, H. Chen, Y. Zhao and X. Zeng, *Nat. Commun.*, 2023, **14**, 7658.
6 X. Wang, J. Chang and C. Wu, *Appl. Mater. Today*, 2018, **11**, 308–319.
7 A. G. Kurian, R. K. Singh, V. Sagar, J.-H. Lee and H.-W. Kim, *Nano-Micro Lett.*, 2024, **16**, 110.
8 B. Magne, A. Demers, É. Savard, M. Lemire-Rondeau, N. Veillette, V. Pruneau, R. Guignard, A. Morissette, D. Larouche, F. A. Auger and L. Germain, *Acta Biomater.*, 2023, **167**, 249–259.
9 K. Kang, S. Ye, C. Jeong, J. Jeong, Y.-S. Ye, J.-Y. Jeong, Y.-J. Kim, S. Lim, T. H. Kim, K. Y. Kim, J. U. Kim, G. I. Kim, D. H. Chun, K. Kim, J. Park, J.-H. Hong, B. Park, K. Kim, S. Jung, K. Baek, D. Cho, J. Yoo, K. Lee, H. Cheng, B.-W. Min, H. J. Kim, H. Jeon, H. Yi, T.-I. Kim, K. J. Yu and Y. Jung, *Nat. Commun.*, 2024, **15**, 10.
10 C. Gao, L. Zhang, J. Wang, M. Jin, Q. Tang, Z. Chen, Y. Cheng, R. Yang and G. Zhao, *J. Mater. Chem. B*, 2021, **9**, 3106–3130.
11 P. I. Campa-Siqueiros, T. J. Madera-Santana, M. M. Castillo-Ortega, J. Lopez-Cervantes, J. F. Ayala-Zavala and E. L. Ortiz-Vazquez, *RSC Adv.*, 2021, **11**, 15340–15350.
12 J. Xue, T. Wu, Y. Dai and Y. Xia, *Chem. Rev.*, 2019, **119**, 5298–5415.
13 K. R. S. Dinuwan Gunawardhana, R. B. V. B. Simorangkir, G. B. McGuinness, M. S. Rasel, L. A. Magre Colorado, S. S. Baberwal, T. E. Ward, B. O'Flynn and S. M. Coyle, *ACS Nano*, 2024, **18**, 2649–2684.
14 Z. Dong, Q. Liu, X. Han, X. Zhang, X. Wang, C. Hu, X. Li, J. Liang, Y. Chen and Y. Fan, *J. Mater. Chem. B*, 2023, **11**, 6346–6360.
15 K. A. Rieger, N. P. Birch and J. D. Schiffman, *J. Mater. Chem. B*, 2013, **1**, 4531–4541.
16 A. Keirouz, M. Chung, J. Kwon, G. Fortunato and N. Radacsi, *Wiley Interdiscip. Rev.: Nanomed. Nanobiotechnol.*, 2020, **12**, e1626.
17 Z. Huang, H. An, H. Guo, S. Ji, Q. Gu, Z. Gu and Y. Wen, *Adv. Fiber Mater.*, 2024, DOI: **10.1007/s42765-023-00364-7**.
18 X. Han, L. Wang, Y. Shang, X. Liu, J. Yuan and J. Shen, *J. Mater. Chem. B*, 2022, **10**, 8672–8683.
19 E. Hosseini-Alvand and M.-T. Khorasani, *J. Mater. Chem. B*, 2023, **11**, 890–904.
20 T. L. Braga, A. R. de Souza Rossin, J. A. Fernandes, P. de Souza Bonfim de Mendonça, L. V. de Castro-Hoshino, M. L. Baesso, C. F. de Freitas, E. Radovanovic and W. Caetano, *Appl. Mater. Today*, 2024, **36**, 102073.
21 Y. Hou, X. Xu, Y. Zhou, Q. Li, L. Zhu, C. Liu, S. Chen and J. Pang, *ACS Appl. Mater. Interfaces*, 2024, **16**, 8228–8237.
22 X. Li, L. Pattelli, Z. Ding, M. Chen, T. Zhao, Y. Li, H. Xu, L. Pan and J. Zhao, *Adv. Funct. Mater.*, 2024, 2315315.
23 W. He, C. Li, S. Zhao, Z. Li, J. Wu, J. Li, H. Zhou, Y. Yang, Y. Xu and H. Xia, *Bioact. Mater.*, 2024, **34**, 338–353.
24 D.-G. Yu, X.-Y. Li, X. Wang, J.-H. Yang, S. W. A. Bligh and G. R. Williams, *ACS Appl. Mater. Interfaces*, 2015, **7**, 18891–18897.
25 T. Zhao, Y. Zheng, X. Zhang, D. Teng, Y. Xu and Y. Zeng, *Mater. Des.*, 2021, **205**, 109705.
26 J. Yin, L. Xu and A. Ahmed, *Adv. Fiber Mater.*, 2022, **4**, 832–844.
27 J. Zhou, T. Yi, Z. Zhang, D.-G. Yu, P. Liu, L. Wang and Y. Zhu, *Adv. Compos. Hybrid Mater.*, 2023, **6**, 189.
28 Z. Xu, J. Fan, W. Tian, X. Ji, Y. Cui, Q. Nan, F. Sun and J. Zhang, *Adv. Funct. Mater.*, 2023, **34**, 2307449.
29 J. Li, Q. Du, J. Wan, D.-G. Yu, F. Tan and X. Yang, *Mater. Des.*, 2024, **238**, 112657.
30 L. Liu, H. Sun, J. Zhang, B. Xu, Y. Gao, D. Qi, Z. Mao and J. Wu, *Adv. Fiber Mater.*, 2022, **5**, 574–587.
31 E. Mele, *J. Mater. Chem. B*, 2016, **4**, 4801–4812.
32 D. Ji, Y. Lin, X. Guo, B. Ramasubramanian, R. Wang, N. Radacsi, R. Jose, X. Qin and S. Ramakrishna, *Nat. Rev. Methods Primers*, 2024, **4**, 1.
33 Y. Si, S. Shi and J. Hu, *Nano Today*, 2023, **48**, 101723.
34 M. Tarnowska, S. Briancon, J. Resende de Azevedo, Y. Chevalier and M. A. Bolzinger, *Int. J. Pharm.*, 2020, **591**, 119991.
35 M. A. Zoroddu, J. Aaseth, G. Crisponi, S. Medici, M. Peana and V. M. Nurchi, *J. Inorg. Biochem.*, 2019, **195**, 120–129.
36 N. Ninan, M. Muthiah, I.-K. Park, T. W. Wong, S. Thomas and Y. Grohens, *Polym. Rev.*, 2015, **55**, 453–490.
37 X. Yang, J. Yang, L. Wang, B. Ran, Y. Jia, L. Zhang, G. Yang, H. Shao and X. Jiang, *ACS Nano*, 2017, **11**, 5737–5745.
38 J. Yang, K. Wang, D. G. Yu, Y. Yang, S. W. A. Bligh and G. R. Williams, *Mater. Sci. Eng., C*, 2020, **111**, 110805.
39 B. Suganya Bharathi and T. Stalin, *Mater. Today Commun.*, 2019, **21**, 100664.
40 S. Pina, J. M. Oliveira and R. L. Reis, *Adv. Mater.*, 2015, **27**, 1143–1169.
41 K. E. Mosaad, K. R. Shoueir and M. M. Dewidar, *J. Cluster. Sci.*, 2021, 1–12.
42 X. Chen, X. Ge, Y. Qian, H. Tang, J. Song, X. Qu, B. Yue and W. E. Yuan, *Adv. Funct. Mater.*, 2020, **30**, 2004537.
43 L. Dong, M. Ren, Y. Wang, G. Wang, S. Zhang, X. Wei, J. He, B. Cui, Y. Zhao, P. Xu, X. Wang, J. Di and Q. Li, *Sci. Adv.*, 2022, **8**, eabq7703.
44 H. Jiang, L. Wang and K. Zhu, *J. Controlled Release*, 2014, **193**, 296–303.
45 Z. Mahdieh, S. Mitra and A. Holian, *ACS Appl. Polym. Mater.*, 2020, **2**, 4004–4015.
46 Y. Sun, S. Cheng, W. Lu, Y. Wang, P. Zhang and Q. Yao, *RSC Adv.*, 2019, **9**, 25712–25729.

47 J. Yoon, H. S. Yang, B. S. Lee and W. R. Yu, *Adv. Mater.*, 2018, **30**, e1704765.
48 P. J. Rivero, A. Urrutia, J. Goicoechea, Y. Rodríguez, J. M. Corres, F. J. Arregui and I. R. Matías, *J. Appl. Polym. Sci.*, 2012, **126**, 1228–1235.
49 Q. Li, Y. Yin, D. Cao, Y. Wang, P. Luan, X. Sun, W. Liang and H. Zhu, *ACS Nano*, 2021, **15**, 11992–12005.
50 C. S. Chen, M. Mrksich, S. Huang, G. M. Whitesides and D. E. Ingber, *Science*, 1997, **276**, 1425–1428.
51 J. M. Gao, X. Y. Yu, X. L. Wang, Y. N. He and J. D. Ding, *Engineering*, 2022, **13**, 31–45.
52 R. Augustine, Y. B. Dalvi, V. K. Y. Nath, R. Varghese, V. Raghuveeran, A. Hasan, S. Thomas and N. Sandhyarani, *Mater. Sci. Eng., C*, 2019, **103**, 109801.
53 S. Wang, J. Li, Z. Zhou, S. Zhou and Z. Hu, *Molecules*, 2018, **24**, 75.
54 Y. T. Wang, T. Ying, J. X. Li, Y. F. Xu, R. Q. Wang, Q. F. Ke, S. G. F. Shen, H. Xu and K. L. Lin, *Chem. Eng. J.*, 2020, **402**, 126273.
55 P. J. Zhang, Y. Q. Jiang, D. Liu, Y. Liu, Q. F. Ke and H. Xu, *Nanomedicine*, 2020, **15**, 2241–2254.
56 Q. Yu, Y. Han, X. Wang, C. Qin, D. Zhai, Z. Yi, J. Chang, Y. Xiao and C. Wu, *ACS Nano*, 2018, **12**, 2695–2707.
57 H. Xu, F. Lv, Y. Zhang, Z. Yi, Q. Ke, C. Wu, M. Liu and J. Chang, *Nanoscale*, 2015, **7**, 18446–18452.
58 F. Lv, J. Wang, P. Xu, Y. Han, H. Ma, H. Xu, S. Chen, J. Chang, Q. Ke, M. Liu, Z. Yi and C. Wu, *Acta Biomater.*, 2017, **60**, 128–143.
59 Z. Zhang, W. Li, Y. Liu, Z. Yang, L. Ma, H. Zhuang, E. Wang, C. Wu, Z. Huan, F. Guo and J. Chang, *Bioact. Mater.*, 2021, **6**, 1910–1920.
60 A. Ullah, A. A. Mamun, M. B. Zaidi, T. Roome and A. Hasan, *Biomed. Pharmacother.*, 2023, **165**, 115156.
61 M. Zehra, W. Zubairi, A. Hasan, H. Butt, A. Ramzan, M. Azam, A. Mehmood, M. Falahati, A. A. Chaudhry, I. U. Rehman and M. Yar, *Int. J. Nanomed.*, 2020, **15**, 3511–3522.
62 Y. Cui, Z. Huang, L. Lei, Q. Li, J. Jiang, Q. Zeng, A. Tang, H. Yang and Y. Zhang, *Nat. Commun.*, 2021, **12**, 5922.
63 S. Nasser, M. Ibrahim and Y. Atassi, *Mater. Chem. Phys.*, 2021, **267**, 124686.
64 X. R. Yu, Z. C. Gao, J. X. Mu, H. Lian and Z. X. Meng, *Biomater. Sci.*, 2023, **11**, 2158–2166.
65 M. Delyanee, A. Solouk, S. Akbari and M. J. Daliri, *Macromol. Biosci.*, 2022, **22**, e2100313.
66 R. Augustine, A. Hasan, N. K. Patan, Y. B. Dalvi, R. Varghese, A. Antony, R. N. Unni, N. Sandhyarani and A.-E. A. Moustafa, *ACS Biomater. Sci. Eng.*, 2019, **6**, 58–70.
67 F. Zhou, C. J. Cui, S. B. Sun, S. H. Wu, S. J. Chen, J. W. Ma and C. M. Li, *Carbohydr. Polym.*, 2022, **282**, 119131.
68 L. Yin, Q. Tang, Q. Ke, X. Zhang, J. Su, H. Zhong and L. Fang, *ACS Appl. Mater. Interfaces*, 2023, **15**, 48903–48912.
69 R. Augustine, S. K. Nethi, N. Kalarikkal, S. Thomas and C. R. Patra, *J. Mater. Chem. B*, 2017, **5**, 4660–4672.
70 S. Zhang, J. Ye, Y. Sun, J. Kang, J. Liu, Y. Wang, Y. Li, L. Zhang and G. Ning, *Chem. Eng. J.*, 2020, **390**, 124523.
71 S. Enoch and D. J. Leaper, *Surgery*, 2008, **26**, 31–37.
72 J. R. Dias, P. L. Granja and P. J. Bártolo, *Prog. Mater. Sci.*, 2016, **84**, 314–334.
73 B. Guo, R. Dong, Y. Liang and M. Li, *Nat. Rev. Chem.*, 2021, **5**, 773–791.
74 Y. Yang, Y. Du, J. Zhang, H. Zhang and B. Guo, *Adv. Fiber Mater.*, 2022, **4**, 1027–1057.
75 Y. Zheng, W. Ma, Z. Yang, H. Zhang, J. Ma, T. Li, H. Niu, Y. Zhou, Q. Yao, J. Chang, Y. Zhu and C. Wu, *Chem. Eng. J.*, 2022, **430**, 132912.
76 Y. Feng, Y. He, X. Lin, M. Xie, M. Liu and Y. Lvov, *Adv. Healthcare Mater.*, 2022, **12**, 2202265.
77 Y. Feng, X. Luo, F. Wu, H. Z. Liu, E. Y. Liang, R. R. He and M. X. Liu, *Chem. Eng. J.*, 2022, **428**, 132049.
78 X. Sun, Z. Tang, M. Pan, Z. Wang, H. Yang and H. Liu, *Carbohydr. Polym.*, 2017, **177**, 135–143.
79 X. X. Wang, Q. Liu, J. X. Sui, S. Ramakrishna, M. Yu, Y. Zhou, X. Y. Jiang and Y. Z. Long, *Adv. Healthcare Mater.*, 2019, **8**, e1900823.
80 S. Y. Ong, J. Wu, S. M. Moochhala, M. H. Tan and J. Lu, *Biomaterials*, 2008, **29**, 4323–4332.
81 K. H. Nam, E. Yeom, H. Ha and S. J. Lee, *Ultrasound Med. Biol.*, 2012, **38**, 468–475.
82 M. Delyanee, A. Solouk, S. Akbari and M. Daliri Joupari, *Polym. Adv. Technol.*, 2021, **32**, 3934–3947.
83 R. N. Udangawa, P. E. Mikael, C. Mancinelli, C. Chapman, C. F. Willard, T. J. Simmons and R. J. Linhardt, *ACS Appl. Mater. Interfaces*, 2019, **11**, 15447–15456.
84 A. J. Tompeck, A. U. R. Gajdhar, M. Dowling, S. B. Johnson, P. S. Barie, R. J. Winchell, D. King, T. M. Scalea, L. D. Britt and M. Narayan, *J. Trauma Acute Care Surg.*, 2020, **88**, e1–e21.
85 X. Liang, C. Jintao and W. Jiana, *Guangdong Chem. Ind.*, 2018, **45**, 67–69.
86 S. S. Yuan, X. X. Sun, Y. Shen and Z. B. Li, *Macromol. Biosci.*, 2022, **22**, e2100524.
87 K. Madhumathi, P. T. Sudheesh Kumar, S. Abhilash, V. Sreeja, H. Tamura, K. Manzoor, S. V. Nair and R. Jayakumar, *J. Mater. Sci.: Mater. Med.*, 2010, **21**, 807–813.
88 L. A. Alshabanah, M. Hagar, L. A. Al-Mutabagani, G. M. Abozaid, S. M. Abdallah, N. Shehata, H. Ahmed and A. H. Hassanin, *Polymers*, 2021, **13**, 1776.
89 A. A. Hassan, H. A. Radwan, S. A. Abdelaal, N. S. Al-Radadi, M. K. Ahmed, K. R. Shoueir and M. A. Hady, *Int. J. Pharm.*, 2021, **593**, 120143.
90 Z. J. Wang, W. K. Hu, W. Wang, Y. Xiao, Y. Chen and X. H. Wang, *Adv. Fiber Mater.*, 2023, **5**, 107–129.
91 B. Maharjan, M. K. Joshi, A. P. Tiwari, C. H. Park and C. S. Kim, *J. Mech. Behav. Biomed. Mater.*, 2017, **65**, 66–76.
92 A. Haider, S. Kwak, K. C. Gupta and I.-K. Kang, *J. Nanomater.*, 2015, **2015**, 1–10.
93 G. Prado-Prone, P. Silva-Bermudez, A. Almaguer-Flores, J. A. Garcia-Macedo, V. I. Garcia, S. E. Rodil, C. Ibarra and C. Velasquillo, *Nanomedicine*, 2018, **14**, 1695–1706.
94 H. Golipour, E. Ezzatzadeh and A. Sadeghianmaryan, *J. Appl. Polym. Sci.*, 2022, **139**, e52505.

95 E. Ghasemian Lemraski, H. Jahangirian, M. Dashti, E. Khajehali, S. Sharafinia, R. Rafiee-Moghaddam and T. J. Webster, *Int. J. Nanomed.*, 2021, **16**, 223–235.
96 H. Chen, J. Zhang, H. Wu, Y. Li, X. Li, J. Zhang, L. Huang, S. Deng, S. Tan and X. Cai, *ACS Appl. Bio Mater.*, 2021, **4**, 6137–6147.
97 M. Bandeira, B. S. Chee, R. Frassini, M. Nugent, M. Giovanela, M. Roesch-Ely, J. D. S. Crespo and D. M. Devine, *Materials*, 2021, **14**, 2889.
98 R. Ahmed, M. Tariq, I. Ali, R. Asghar, P. Noorunnisa Khanam, R. Augustine and A. Hasan, *Int. J. Biol. Macromol.*, 2018, **120**, 385–393.
99 S. D. Wang, Q. Ma, K. Wang and H. W. Chen, *ACS Omega*, 2018, **3**, 406–413.
100 K. Ghosal, C. Agatemor, Z. Špitálsky, S. Thomas and E. Kny, *Chem. Eng. J.*, 2019, **358**, 1262–1278.
101 T. V. Toniatto, B. V. M. Rodrigues, T. C. O. Marsi, R. Ricci, F. R. Marciano, T. J. Webster and A. O. Lobo, *Mater. Sci. Eng., C*, 2017, **71**, 381–385.
102 D. Archana, J. Dutta and P. K. Dutta, *Int. J. Biol. Macromol.*, 2013, **57**, 193–203.
103 K. Ghosal, A. Manakhov, L. Zajickova and S. Thomas, *AAPS PharmSciTech*, 2017, **18**, 72–81.
104 W.-C. Jao, M.-C. Yang, C.-H. Lin and C.-C. Hsu, *Polym. Adv. Technol.*, 2012, **23**, 1066–1076.
105 L. Yan, S. Si, Y. Chen, T. Yuan, H. Fan, Y. Yao and Q. Zhang, *Fibers Polym.*, 2011, **12**, 207–213.
106 D. Archana, B. K. Singh, J. Dutta and P. K. Dutta, *Carbohydr. Polym.*, 2013, **95**, 530–539.
107 M. S. Al Mogbel, M. T. Elabbasy, R. S. Mohamed, A. E. Ghoniem, M. F. H. A. El-Kader and A. A. Menazea, *J. Polym. Res.*, 2021, **28**, 1–8.
108 H. Zhang, Z. Xu, Y. Mao, Y. Zhang, Y. Li, J. Lao and L. Wang, *Polymers*, 2021, **13**, 3942.
109 S. Wang, F. Yan, P. Ren, Y. Li, Q. Wu, X. Fang, F. Chen and C. Wang, *Int. J. Biol. Macromol.*, 2020, **158**, 9–17.
110 C. Pettinari, R. Pettinari, C. Di Nicola, A. Tombesi, S. Scuri and F. Marchetti, *Coord. Chem. Rev.*, 2021, **446**, 214121.
111 A. Saatchi, A. R. Arani, A. Moghanian and M. Mozafari, *Ceram. Int.*, 2021, **47**, 9447–9461.
112 G. S. Liu, X. Yan, F. F. Yan, F. X. Chen, L. Y. Hao, S. J. Chen, T. Lou, X. Ning and Y. Z. Long, *Nanoscale Res. Lett.*, 2018, **13**, 309.
113 F. Ciftci, S. Ayan, N. Duygulu, Y. Yilmazer, Z. Karavelioglu, M. Vehapi, R. Cakır Koc, M. Sengor, H. Yılmazer, D. Ozcimen, O. Gunduz and C. B. Ustundag, *Int. J. Polym. Mater. Polym. Biomater.*, 2021, **71**, 1–12.
114 K. Santiago-Castillo, A. M. Torres-Huerta, D. Del Angel-Lopez, M. A. Dominguez-Crespo, H. Dorantes-Rosales, D. Palma-Ramirez and H. Willcock, *Polymers*, 2022, **14**, 674.
115 R. Li, Z. Cheng, X. Yu, S. Wang, Z. Han and L. Kang, *Mater. Lett.*, 2019, **254**, 206–209.
116 S. Calamak, E. A. Aksoy, N. Ertas, C. Erdogdu, M. Sagıroglu and K. Ulubayram, *Eur. Polym. J.*, 2015, **67**, 99–112.
117 M. M. Fouda, M. R. El-Aassar and S. S. Al-Deyab, *Carbohydr. Polym.*, 2013, **92**, 1012–1017.
118 A. M. Abdelgawad, S. M. Hudson and O. J. Rojas, *Carbohydr. Polym.*, 2014, **100**, 166–178.
119 I. V. Lukiev, L. S. Antipina, S. I. Goreninskii, T. S. Tverdokhlebova, D. V. Vasilchenko, A. L. Nemoykina, D. A. Goncharova, V. A. Svetlichnyi, G. T. Dambaev, V. M. Bouznik and E. N. Bolbasov, *Membranes*, 2021, **11**, 986.
120 G. Q. Blantocas, A. S. Alaboodi and A.-b H. Mekky, *Arabian J. Sci. Eng.*, 2017, **43**, 389–398.
121 M. Salehi, K. Shahporzadeh, A. Ehterami, H. Yeganehfard, H. Ziaei, M. M. Azizi, S. Farzamfar, A. Tahersoltani, A. Goodarzi, J. Ai and A. Ahmadi, *Fibers Polym.*, 2020, **21**, 1713–1721.
122 B. Dalisson and J. Barralet, *Adv. Healthcare Mater.*, 2019, **8**, e1900764.
123 U. Dashdorj, M. K. Reyes, A. R. Unnithan, A. P. Tiwari, B. Tumurbaatar, C. H. Park and C. S. Kim, *Int. J. Biol. Macromol.*, 2015, **80**, 1–7.
124 Y. Zhang, M. Chang, F. Bao, M. Xing, E. Wang, Q. Xu, Z. Huan, F. Guo and J. Chang, *Nanoscale*, 2019, **11**, 6315–6333.
125 E. Fallahiarezoudar, M. Ahmadipourroudposht, A. Idris, N. M. Yusof, M. Marvibaigi and M. Irfan, *J. Mater. Sci.*, 2016, **51**, 8361–8381.
126 S. Chen, Z. Huan, L. Zhang and J. Chang, *Int. J. Surg.*, 2018, **52**, 229–232.
127 X. Wang, F. Lv, T. Li, Y. Han, Z. Yi, M. Liu, J. Chang and C. Wu, *ACS Nano*, 2017, **11**, 11337–11349.
128 Y. Lv, Y. Xu, X. Sang, C. Li, Y. Liu, Q. Guo, S. Ramakrishna, C. Wang, P. Hu and H. S. Nanda, *J. Mater. Chem. B*, 2022, **10**, 1116–1127.
129 Q. Chen, J. Wu, Y. Liu, Y. Li, C. Zhang, W. Qi, K. W. K. Yeung, T. M. Wong, X. Zhao and H. Pan, *Mater. Sci. Eng., C*, 2019, **105**, 110083.
130 X. Zhang, Y. Li, Z. Ma, D. He and H. Li, *Bioact. Mater.*, 2021, **6**, 3692–3704.
131 J. Li, F. Lv, H. Xu, Y. Zhang, J. Wang, Z. Yi, J. Yin, J. Chang and C. Wu, *J. Mater. Chem. B*, 2017, **5**, 1926–1934.
132 M. Liu, R. Wang, J. Liu, W. Zhang, Z. Liu, X. Lou, H. Nie, H. Wang, X. Mo, A. I. Abd-Elhamid, R. Zheng and J. Wu, *Biomater. Adv.*, 2022, **133**, 112609.
133 A. P. Veith, K. Henderson, A. Spencer, A. D. Sligar and A. B. Baker, *Adv. Drug Delivery Rev.*, 2019, **146**, 97–125.
134 P. Gao, B. Fan, X. Yu, W. Liu, J. Wu, L. Shi, D. Yang, L. Tan, P. Wan, Y. Hao, S. Li, W. Hou, K. Yang, X. Li and Z. Guo, *Bioact. Mater.*, 2020, **5**, 680–693.
135 C. Zhu, R. Cao, Y. Zhang and R. Chen, *Front. Cell Dev. Biol.*, 2021, **9**, 660571.
136 P. K. Chandra, C. L. Ross, L. C. Smith, S. S. Jeong, J. Kim, J. J. Yoo and B. S. Harrison, *Wound Repair Regen.*, 2015, **23**, 830–841.
137 Y. Hua and G. Bergers, *Front. Immunol.*, 2019, **10**, 2178.
138 L. W. Fu, Q. Feng, Y. J. Chen, J. Z. Fu, X. J. Zhou and C. L. He, *Adv. Fiber Mater.*, 2022, **4**, 1334–1356.
139 Z. Tu, M. Chen, M. Wang, Z. Shao, X. Jiang, K. Wang, Z. Yao, S. Yang, X. Zhang, W. Gao, C. Lin, B. Lei and C. Mao, *Adv. Funct. Mater.*, 2021, **31**, 2100924.

140 J. Hu, T. Wei, H. Zhao, M. Chen, Y. Tan, Z. Ji, Q. Jin, J. Shen, Y. Han, N. Yang, L. Chen, Z. Xiao, H. Zhang, Z. Liu and Q. Chen, *Matter*, 2021, **4**, 2985–3000.
141 R. Yunus Basha, T. S. Sampath Kumar, R. Selvaraj and M. Doble, *Macromol. Mater. Eng.*, 2018, **303**, 1800234.
142 H. A. Rather, R. Thakore, R. Singh, D. Jhala, S. Singh and R. Vasita, *Bioact. Mater.*, 2018, **3**, 201–211.
143 J. Sun, W. Jia, H. Qi, J. Huo, X. Liao, Y. Xu, J. Wang, Z. Sun, Y. Liu, J. Liu, M. Zhen, C. Wang and C. Bai, *Adv. Mater.*, 2024, 2312440.
144 R. Goldman, *Adv. Skin Wound Care*, 2004, **17**, 24–35.
145 C. K. Sen, S. Khanna, B. M. Babior, T. K. Hunt, E. C. Ellison and S. Roy, *J. Biol. Chem.*, 2002, **277**, 33284–33290.
146 H. Wu, F. Li, S. Wang, J. Lu, J. Li, Y. Du, X. Sun, X. Chen, J. Gao and D. Ling, *Biomaterials*, 2018, **151**, 66–77.
147 A. Pellicoro, P. Ramachandran, J. P. Iredale and J. A. Fallowfield, *Nat. Rev. Immunol.*, 2014, **14**, 181–194.
148 J. Li, F. Lv, J. Li, Y. Li, J. Gao, J. Luo, F. Xue, Q. Ke and H. Xu, *Nano Res.*, 2020, **13**, 2268–2279.
149 S. Faraji, N. Nowroozi, A. Nouralishahi and J. Shabani Shayeh, *Life Sci.*, 2020, **257**, 118062.
150 D. Li, W. Nie, L. Chen, Y. Miao, X. Zhang, F. Chen, B. Yu, R. Ao, B. Yu and C. He, *RSC Adv.*, 2017, **7**, 7973–7982.
151 A. Arno, A. H. Smith, P. H. Blit, M. A. Shehab, G. G. Gauglitz and M. G. Jeschke, *Pharmaceuticals*, 2011, **4**, 1355–1380.
152 S. He, L. Wu, X. Li, H. Sun, T. Xiong, J. Liu, C. Huang, H. Xu, H. Sun, W. Chen, R. Gref and J. Zhang, *Acta Pharm. Sin. B*, 2021, **11**, 2362–2395.
153 E. Lamei and M. Hasanzadeh, *Int. J. Biol. Macromol.*, 2022, **208**, 409–420.
154 S. Yang, X. Zhang and D. Zhang, *Int. J. Mol. Sci.*, 2019, **20**, 4395.
155 Y. Jia, H. Zhang, S. Yang, Z. Xi, T. Tang, R. Yin and W. Zhang, *Nanomedicine*, 2018, **13**, 2881–2899.
156 Z. Song, Y. Ma, G. Xia, Y. Wang, W. Kapadia, Z. Sun, W. Wu, H. Gu, W. Cui and X. Huang, *J. Mater. Chem. B*, 2017, **5**, 7632–7643.
157 S. Rathinavel, P. S. Korrapati, P. Kalaiselvi and S. Dharmalingam, *Eur. J. Pharm. Sci.*, 2021, **167**, 106021.
158 J. Jalvandi, M. White, Y. B. Truong, Y. Gao, R. Padhye and I. L. Kyratzis, *J. Mater. Sci.*, 2015, **50**, 7967–7974.
159 J. Sun, Y. Fan, P. Zhang, X. Zhang, Q. Zhou, J. Zhao and L. Ren, *J. Colloid Interface Sci.*, 2020, **559**, 197–205.
160 R. H. Dong, Y. X. Jia, C. C. Qin, L. Zhan, X. Yan, L. Cui, Y. Zhou, X. Jiang and Y. Z. Long, *Nanoscale*, 2016, **8**, 3482–3488.
161 S. Qian, L. Song, L. Sun, X. Zhang, Z. Xin, J. Yin and S. Luan, *J. Photochem. Photobiol., A*, 2020, **400**, 112626.
162 S. Zirak Hassan Kiadeh, A. Ghaee, M. Farokhi, J. Nourmohammadi, A. Bahi and F. K. Ko, *Int. J. Biol. Macromol.*, 2021, **173**, 351–365.
163 P. Zhang, Y. Li, Y. Tang, H. Shen, J. Li, Z. Yi, Q. Ke and H. Xu, *ACS Appl. Mater. Interfaces*, 2020, **12**, 18319–18331.

